BROADBAND INCOHERENT IMAGING USING MULTIPLE APERTURE OPTICS

THESIS

Konrad S. Gruca
Major, USAF

AFIT/GSO/ENP/89D-3

DEPARTMENT OF THE AIR FORCE
AIR UNIVERSITY
AIR FORCE INSTITUTE OF TECHNOLOGY

Wright-Patterson Air Force Base, Ohio

AFIT/GSO/ENP/87D-3

BROADBAND INCOHERENT IMAGING USING MULTIPLE APERTURE OPTICS

THESIS

Presented to the Faculty of the School of Engineering
of the Air Force Institute of Technology
Air University
In Partial Fulfillment of the
Requirements for the Degree of
Master of Science in Space Operations

Konrad S. Gruca, B.S.
Major, USAF

December 1989

Preface

Due to size and weight restrictions on launching telescopes into space, the concept of multiple mirror telescopes must be vigorously pursued. This thesis involves taking several multiple mirror configurations and, by using information gathered at several wavelengths, increasing the resolving capability of each particular system without adding more or larger mirrors to the system. The only weight addition would be the additional sensors needed to detect the light at multiple wavelengths. There were seven configurations studied; some allowed for a marked increase in resolution, others did not. This thesis presents the optimum solution found for six of the mirror configuration studied.

I would like to thank Capt Jim Targove for his constant and patient guidance as the advisor throughout this effort. I also thank Maj Bruce Morlan for his contributions to the Operations Research optimization portion of this effort; his help in starting the optimization computer code was invaluable. Last, but certainly not least, I thank my wife, Danusia, for her endless patience and understanding throughout the trials and tribulations of the past eighteen months.

Konrad S. Gruca

Table of Contents

	page
Preface	ii
List of Figures	v
List of Tables	vii
Abstract	viii
I. Background	1
Introduction	1
Problem Statement	2
Literature Review	2
Single Mirror Telescopes	3
Multiple Mirror Telescopes	4
Spatial Resolution and Modulation Transfer Function (MTF)	7
Synthetic Aperture Diameter	11
Multiple Mirror Geometry	12
Thesis Objectives	13
II. Theory	17
Introduction	17
Pupil Function	17
Fourier Transforms and Optics	19
Point Spread Function	21
Autocorrelation of the Cylinder Function	22
Optical Transfer Function and Modulation Transfer Function	23
Determining Significance of Increase in Resolution	26
Optimization	28
III. Methodology	31
Introduction	31
Graphical Representation of the MTF	31
Computer Routines	39
Determining Optimum Configuration	40
Comparison of Mirror Systems	43
Determining Resolution Increase Significance	44
Optimization	45
IV. Results	49
Introduction	49
General Observations	49
Odd Mirror Symmetrical Systems	50
Golay Configurations	51
Operations Research Optimizations	51

page

Detailed Results 52
Three-Mirror Equilateral Triangle 53
Four-Mirror Cross 55
Four-Mirror Cross with Center Mirror 58
Five-Mirror Pentagon 58
Six-Mirror Configurations 61
Qualitative Comparison of Golay 6 Resolution . . . 66

V. Conclusions 69

Summary 69
General Conclusions 70
Recommendations 71

APPENDIX A: Main Program used in Generating MTF 72

APPENDIX B: Code to Write Input for Main Program 74

APPENDIX C: Optimization Code 75

APPENDIX D: Coordinates of Mirror Systems 80

APPENDIX E 84

Bibliography 87

Vita 89

List of Figures

Figure		page
1.	Imagery of a bar target	8
2.	Determine the modulation of a test pattern	9
3.	Image modulation vs frequency of the test pattern	9
4.	Mirror geometries	16
5.	Cylinder function	19
6.	Simple thin lens imaging	27
7.	MTF of a one mirror system	33
8.	Four Mirror MTF plots	34
9.	Three- and five-micron 3-dimensional plots	36
10.	Three- and five-micron contour plots	37
11.	Contour plots of four mirror pupil at various mirror distances	38
12.	Contour plot showing interior zero	39
13.	MTF as radius increases	42
14.	MTF of optimum four mirror cross at three to five microns wavelength	43
15.	Four-mirror Golay	52
16.	3-Mirror triangle	54
17.	3-mirror, 3-micron MTF	54
18.	3-mirror, 3-5 micron MTF	54
19.	4-mirror box	56
20.	4-mirror box, 3 micron 3-D plot	56
21.	4-mirror box, 3 micron contour plot	56
22.	4-mirror box, 3-5 micron contour plot	56
23.	4-mirror OR optimum, 3-micron	57
24.	4 mirror OR optimum, 3 micron contour plot	57

Figure page

25. 4-mirror OR optimum , 3-5 micron 57
26. 4-mirror OR optimum, 3-5 micron contour plot . . 57
27. 5-mirror pentagon 60
28. 5-mirror pentagon, 3 micron contour plot 60
29. 5-mirror pentagon, 3-5 micron contour plot . . . 60
30. 5-mirror OR optimum, 3-5 micron contour plot . . 60
31. 6-mirror hexagon 63
32. 6-mirror hexagon, 3 micron 3-D plot 63
33. 6-mirror hexagon, 3 micron contour plot 63
34. 6-mirror hexagon, 3-5 micron contour plot . . . 63
35. 6-mirror Golay 64
36. 6-mirror Golay, 3 micron 3-D plot 64
37. 6-mirror Golay, 3 micron contour plot 64
38. 6-mirror Golay, 3-5 micron contour plot 64
39. 6-mirror OR optimum, 3 micron 65
40. 6-mirror OR optimum, 3 micron contour plot . . . 65
41. 6-mirror OR optimum, 3-5 micron 65
42. 6-mirror OR optimum, 3-5 micron contour plot . . 65
43. Comparison of two Golay 6 cylinder cross-sections 67
44. Comparison of Golay 6 3 and 3-5 micron MTF . . . 68

List of Tables

Table		page
1.	Three-Mirror Results	53
2.	Four-Mirror Results	55
3.	Comparison of 4 vs 5 mirror cross	58
4.	5-mirror results	59
5.	Comparison of hexagon and OR optima	62
6.	Comparison of hexagon and Golay optima	62
7.	Comparison of OR and Golay optima	62
8.	3-mirror equilateral triangle	80
9.	Symmetrical optimum 4 mirror cross, 3 micron	81
10.	OR optimum 4-mirror, 3 micron	81
11.	Symmetrical 4-mirror cross, 3 micron	81
12.	OR optimum 4-mirror, 3-5 micron	81
13.	Symmetrical 4-mirror cross with center mirror, 3 micron	81
14.	Symmetrical 4-mirror cross with center mirror, 3-5 micron	81
15.	5-mirror pentagon	82
16.	5-mirror OR optimum, 3-5 micron	82
17.	6-mirror hexagon, 3 micron	82
18.	6-mirror OR optimum, 3 micron	82
19.	6-mirror Golay, 3 micron	82
20.	6-mirror hexagon, 3-5 micron	83
21.	6-mirror OR optimum, 3-5 micron	83
22.	6-mirror Golay, 3-5 micron	83
23.	OR optimized Golay 6, 3 micron	83
24.	OR optimized Golay 6, 3-5 micron	83

Abstract

The theoretical resolution of a multiple mirror telescope can be studied through its Modulation Transfer Function (MTF). Using the figure of merit that the mirrors be moved apart in a manner that would maximize the spatial frequency at which the first zero appears in the MTF, this thesis studied the use of MTF information from multiple wavelengths to delay the appearance of an interior zero in the overall MTF. This would allow the mirrors to be moved further apart and thereby increase the frequency at which the first zero appears in the MTF, increasing the resolving capability of the system. Symmetrical configurations from three to six mirrors were studied. Each configuration was initially manually optimized at three microns, then the system was studied at a three to five micron range to see if the MTF information from other wavelengths would delay the appearance of an interior zero in the overall system MTF, thus allowing an increase in the distance between mirrors. An optimization routine was also employed to see if there were other, nonsymmetrical, mirror configurations that could possibly yield a better theoretical resolution than their symmetrical counterparts.

The various findings throughout the research were detailed. The results were presented as a function of increase in theoretical resolution from the single, three

micron wavelength compared to the multiple, three-to five micron wavelength MTF of the system studied. The optimization routine, in general, yielded a small but significant increase in resolution when compared to a symmetrical system with the same number of mirrors.

BROADBAND INCOHERENT IMAGING USING MULTIPLE APERTURE OPTICS

I. Background

Introduction

A telescope's resolving ability can be improved upon in two ways: the first is increasing the diameter of the aperture, and the second is using a phased array optical system. The ability to resolve objects, that is, visually distinguish what an object is, is directly related to the diameter of the optics used in the observation. The greater the diameter of the optics, the better the resolution.

The Hubble telescope (to be launched into space in the near future), has already reached the size limit of any single aperture telescope that can be put into space (11:762). Increasing the diameter of the telescope aperture is not presently feasible because there is no launch platform capable of putting a telescope with a larger diameter into orbit (11:763). Therefore, this thesis considered a more promising second option, a phased array optical system. In this system, the effective diameter of

the telescope can be greatly increased by using several smaller mirrors in a phased array, rather than increasing the size of the single mirror. Another favorable feature of this type of array is reduced cost when compared to a single mirror system with an equivalent diameter (11:763).

Problem Statement

The purpose of this thesis was to investigate the concept of utilizing information gathered at multiple wavelengths in order to improve the theoretical resolving capability of a multiple mirror system. Specifically, it studied seven mirror configurations, varying the geometry and/or the number of mirrors in each. In each multiple mirror system studied, the goal was to use information gathered at multiple wavelengths which could then allow an increase in the distance between mirrors, thereby improving the resolving capability of that system.

Literature Review

The following sections review literature pertinent to this research proposal. Specifically, this discussion covers: the history of optical telescopes, multiple mirror telescopes, spatial resolving power of single versus multiple mirror optics, criteria for determining the effective diameter of single versus multiple mirror optics, the specific problems associated with imaging incoherent light through multiple mirror optical systems, and specific geometries associated with multiple mirror optics (8).

Single Mirror Telescopes. The first recorded use of a telescope for the observation of celestial objects was by Galileo Galilei in the fall of 1609 (3:30). From that day on, the drive has been to improve upon the quality of the received image. Until recently, the primary method of improving resolution has been simply to increase the diameter of the single mirror used in the telescope. The following equation expresses the resolving capability of a telescope:

$$\theta = 1.22 \frac{\lambda}{d} \qquad (1)$$

where θ is the angular separation between two far-field points being observed (in radians), λ is the wavelength of the incident light (in meters), and d is the diameter of the collecting optics (in meters). At this angle, the points are just able to be distinguished as two distinct points. This limit is known as the Rayleigh diffraction limit (5:138). As one surmises from Equation (1), a decrease in wavelength or an increase in the mirror diameter will increase the resolving capability of the system. The operating wavelength range of a telescope system is constrained by the type of information one wishes to study (infrared, microwave, visible, etc.); however, astronomers can easily determine the diameter of the primary mirror when building a telescope, and, the larger the diameter, the better its resolving capability.

However, there are serious drawbacks to building larger mirrors for use in telescopes. One is that

> ...(I)ncreasing the diameter of an optical telescope by simply scaling it up will, from historical experience, increase the cost nearly in proportion to the cube of the ratio of the increased diameter. (11:763)

A second major drawback is the sheer weight of the mirror. Even Galileo realized that there is a limit to the size of a mirror due to weight (3:30). As the weight of the mirror increases, it begins to buckle and warp under its own weight unless massive supports hold it rigid. The astronomical world has nearly reached its limit on size of a traditional monolith mirror with the 5 meter telescope on Mt. Palomar (19:17) and the Russian attempts at a 6 meter mirror (3:30). There is a pressing need to develop new technologies to increase the diameter without paying the tremendous penalties in weight and cost.

Multiple Mirror Telescopes. There is another method to increase the diameter of an optical system -- by using two or more mirrors spaced a distance apart, but synchronized in such a way that the radiation they are receiving is in phase (4:161).

> The term optical phased array describes an optical configuration which is a group of telescopes or imaging systems, each with independent capability, coherently combined to produce a significantly larger aperture optical system. (6:122)

The term "optics" refers to any aperture that collects electromagnetic radiation, such as a radio dish, but is more commonly used to describe the classical mirror telescopes. With the advent of atomic clocks in the 1960s (needed for accurate timekeeping and phase matching), radio astronomy has adapted the method of phasing arrays to increase the receiver's diameter (15:52). The multiple receivers could be as far apart as desired. Even more surprising, if radio astronomers keep an accurate time, they can take observations at 180 day intervals, thus effectively increasing the diameter of the optics to the diameter of the earth's orbit (4:162). This phased array technique for increasing the diameter of the optics works well for radio astronomy, but it is very difficult to adapt to infrared and visible wavelength astronomy because building a synthetic aperture system critically depends on matching the phase of the collected radiation at the receiver.

"The difficulty in synthesizing an aperture lies in achieving and maintaining matched optical paths of several independent optical systems" (7:3). The tolerance must be within fractions of a wavelength (4:163). This phase matching is relatively simple for the radio telescope; the incident radiation wavelength is measured in meters, thus requiring tolerances in centimeters. The wavelengths used in infrared and visible astronomy are measured in microns -- 10^{-6} meters -- thus requiring a tolerance of about 10^{-8} meters. Only recently has control of this incredibly small

tolerance been achieved by coupling computers with lasers to keep the optics aligned within tolerance (17:24). Physics now has a method of increasing the resolving capability of infra-red and visible astronomy without the need for larger single mirror telescopes.

Credit for using the first optical synthetic aperture device goes to Michelson and his two mirror interferometer in the 1920s (6:122), but this was a very specialized application of the multiple aperture device, where detecting the angular separation of two or more stars depended on matching the phase of two stars with two mirrors. "A more recent, truly dramatic demonstration of infrared aperture synthesis was accomplished on the Multiple Mirror Telescope" (6:122), completed in 1979 (19:17). This six-mirror telescope has a mirror diameter of 4.5 meters (nearly the diameter of the Mt Palomar telescope), and was built at a cost roughly one-third that of a conventional single mirror telescope with similar dimensions (3:37).

There are distinct advantages to multiple mirror telescopes.

> Multiple aperture imaging configurations are advantageous for three basic reasons. The first reason is a very practical one -- very high resolution achievable using reasonable optical fabrication methods, cost and schedule...The second phased array advantage is a geometrical one. Arrays can be arranged into configurations that are significantly more compact than equivalent diameter and f-number single aperture systems...The third advantage is that the array may have an intrinsically superior optical performance if it is properly configured. (6:126)

Today, there are many other projects underway to take advantage of these advances in optics. Two of these projects are the United States efforts to build the National New Technology Telescope (NNTT) with a diameter of 15 meters and the European scientific community proposal to build the Very Large Telescope (VLT) with a 16 meter diameter (17:23,24). As the realm of multiple mirror telescopes continues to expand, new questions arise as to whether certain standards that apply to single mirror telescopes apply equally well to the multiple mirror systems. But prior to addressing this issue, a concept of measuring a system's resolving capability, the Modulation Transfer Function (MTF) is defined.

Spatial Resolution and Modulation Transfer Function (MTF). A commonly used method of determining the performance of an optical system is by using a target consisting of alternating light and dark bars of equal width (Figure 1)(20:308).

> ...Several sets of patterns of different spacings are usually imaged by the system under test and the finest set in which the line structure can be discerned is considered to be the limit of resolution of the system, which is expressed as a certain number of lines per millimeter. (20:308-309)

As the lines get narrower, the alternating dark and light bars begin to "wash out", becoming more of a grey than a light and dark -- the system slowly loses its ability to detect the contrast between light and dark.

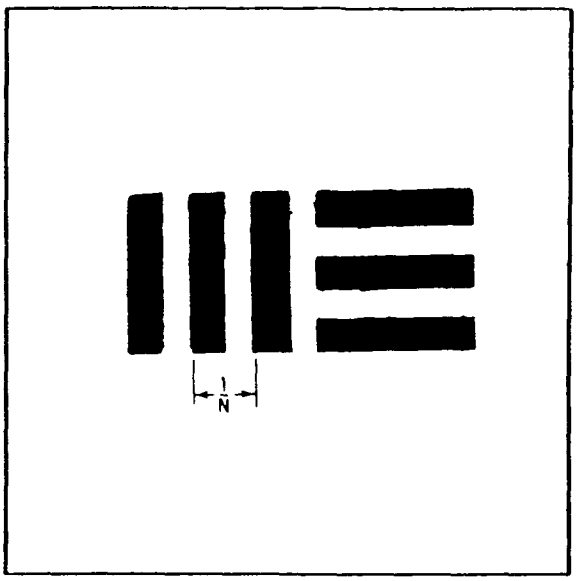

Reprinted from (20:309)

Figure 1. Imagery of a bar target

If we express the contrast in the image as a "modulation", given by the equation

$$\text{MODULATION} = \frac{\text{max} - \text{min}}{\text{max} + \text{min}} \qquad (2)$$

(where max. and min. are as indicated in Fig. 2), we can plot the modulation as a function of the number of lines per millimeter, as indicated in Fig. (3). The intersection of the modulation function line with a horizontal line representing the smallest amount of modulation which the system can detect will give the limiting resolution of the system. (20:310)

The bar target represents the brightness distribution as a square wave. However,

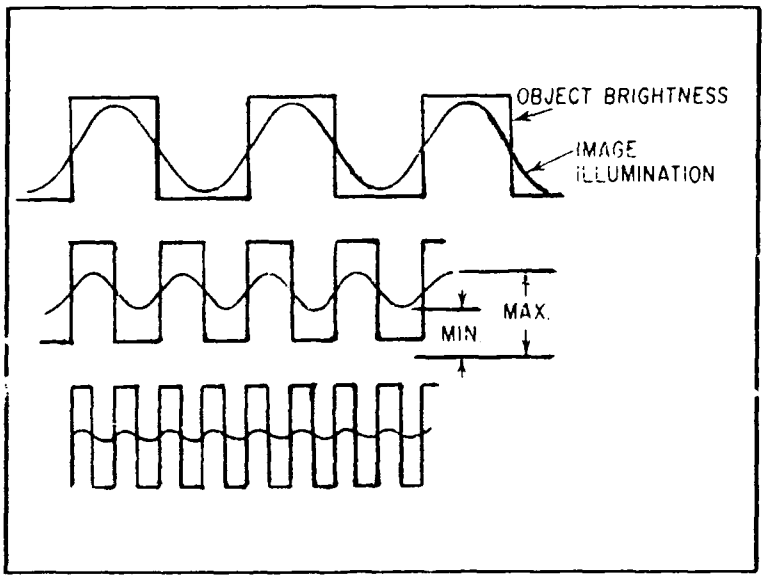

Reprinted from (20:309)

Figure 2. Determining the modulation of a test pattern

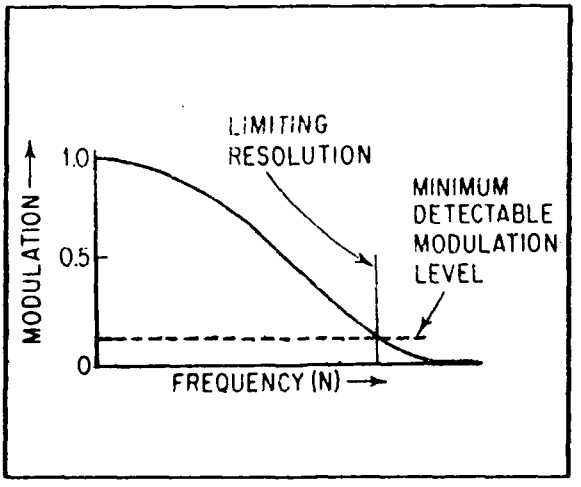

Reprinted from (20:310)

Figure 3. Image modulation vs frequency of the test pattern

> ...if the object pattern is in the form of a sine wave, the distribution in the image is also described by a sine wave, regardless of the shape of the spread function. This fact has led to the widespread use of the Optical Modulation Transfer function to describe the performance of a lens system. The Modulation Transfer Function (MTF) is the ratio of the modulation in the image to that in the object as a function of the frequency (cycles per unit of length) of the sine wave pattern.
>
> $$MTF(\nu) = \frac{M_i}{M_o} \tag{3}$$
>
> A plot of MTF against frequency is thus an almost universally applicable measure of the performance of an image forming system. (20:311)

The discussion to this point has been for a one-dimensional system. To extend the concept of the MTF to two dimensions, one need only to realize that the sine wave pattern can be pointed in any two-dimensional direction. This is analogous to rotating the bar target to any direction over 360^{0}. At any point, these sinusoids can be decomposed into their cartesian components ξ and η with units of (m^{-1}). Just as a one-dimensional waveform, such as a square wave, can be reconstructed using an infinite series of sinusoids (a Fourier transform), a two-dimensional object can be reconstructed using an infinite series of sinusoidal "vectors", the magnitude at any given point as defined by Equation (2).

Simply put, the MTF describes the spatial frequencies that an optical system can and cannot detect, thereby establishing the resolution limit of the system.

> ...While the electronic transfer function describes the ability of a circuit or electrical system to transmit temporal frequencies, the MTF is a description of a system's transmission of spatial frequencies. (18:1)

For the single aperture telescope, the amount of spatial information gathered is a function of the wavelength and mirror diameter -- for a given system configuration, as the wavelength gets shorter and/or the diameter increases, the system can gather higher frequency spatial information, thereby increasing resolution. However, the multiple mirror's geometry as well as the spacing between mirrors within the system also play an important role in the amount and frequency of the spatial information gathered.

Synthetic Aperture Diameter. The standard method for determining the diameter for multiple mirror telescopes is using the minimum diameter circle which will enclose the entire mirror system. Harvey contends that this figure should not necessarily equate to the diameter value used in determining resolution, as in a single mirror system. He defines the effective diameter of a synthetic aperture optical system to be determined by "...the maximum spatial frequency within which no zeros occur in the MTF" (the calculations to determine the "equivalent diameter" are covered in chapter 3) (11:767). This is important when using a multiple mirror system for imaging incoherent objects because this limit determines a system's ability to resolve images. "Incoherent" in this context refers to any

object that has distinct features such as a specific geometrical shape or form. This is in contrast to a coherent object, such as a star, which is a point source of light with no discernable shape. In this thesis, Harvey's criterion for effective diameter will be used to determine the optimum configuration of a multiple mirror optical system at a single wavelength, and will be referred to as the "minimum MTF". By studying the spatial information a system can gather over a wavelength spectrum (3 to 5 microns), the thesis will attempt to increase the system's effective diameter by filling the gaps in the MTF of one wavelength by using spatial information gathered at different wavelengths.

Multiple Mirror Geometry. There are countless ways in which to arrange a multiple mirror system. Once the number of mirrors is chosen, say four, one can arrange the system in a box pattern, a straight line, a triangle with one mirror in the center, and so on. The task is to determine the best configuration for the system based on its application.

Golay, in 1971, described the patterns he felt would maximize the system's capability for gathering spatial information. He presented three series of arrays, each series including unique arrangements using from two to at least ten mirrors (10:272-273). Bunner states, "The non-redundant two dimensional Golay patterns provide the widest spread of aperture that avoids zeros in the optical transfer

function" (2:182). Part of this thesis will study Golay patterns with other mirror arrangements using the same number of mirrors to determine whether the Golay mirror configurations will also maximize a system's diameter using Harvey's criteria of minimum MTF.

Thesis Objectives

The overall objective of this thesis was to examine several mirror configurations, varying both the number of mirrors in the system and their geometries, to obtain the maximum possible spatial frequency value prior to reaching a zero for a given system at both a single wavelength and a wavelength spectrum. The thesis examined systems consisting from three to six mirrors in various geometrical configurations. The following were the sub-objectives.

The first sub-objective was to develop a computer code for generating the MTF of a given mirror configuration. There were many variations to the main code; they will be discussed in the methodology portion of the thesis. Several peripheral programs were written to facilitate entering starting conditions into the main program. The main programs and the peripheral programs are detailed in chapter three and listed in Appendix A and B.

The second sub-objective was to determine a measure of effectiveness for the multiple mirror system. This measure would be the standard measure throughout the thesis when comparing any of the mirror systems, regardless of the configuration of the number of mirrors. The main criterion

used to determine the spatial resolution of a given system was the minimum MTF definition offered by Harvey, that being to maximize the spatial frequency value at which the first zero occurs in the system's MTF pattern (measured radially from the origin) (11:765).

The next sub-objective was to determine the configuration of the systems to be tested. This was done systematically, beginning with a simple three mirror equilateral triangle to get a feel for the way the mirror system translated into its corresponding MTF pattern. Later studies included increasing the number of mirrors to four, five, and concluding with six; as the number of mirrors in the system increased, the possible configurations of the mirrors increased. Symmetrical patterns were chosen for study in the belief that symmetry in the system would yield the optimum configuration for any of the given mirror numbers. The patterns used are shown in figure 4.

The fourth sub-objective was to manually optimize each symmetrical mirror configuration to choose the optimum configuration for the given number of mirrors. Each configuration was optimized at a single wavelength of three microns (this yielded the maximum possible MTF at the wavelength range studied), and then the system was examined at a spectrum of three to five microns to see if any improvement was obtained by using the spectrum spread vs a single wavelength.

The fifth sub-objective was to write an Operations Research style optimization routine and, using the routine, determine if there was a better mirror configuration that would yield a greater MTF than in the manual optimization of symmetrical configurations. The method is the Hook and Jeeves method, and will be described in detail in the next chapter.

The final sub-objective was to determine if the improvement in the MTF using multiple wavelengths was a significant improvement.

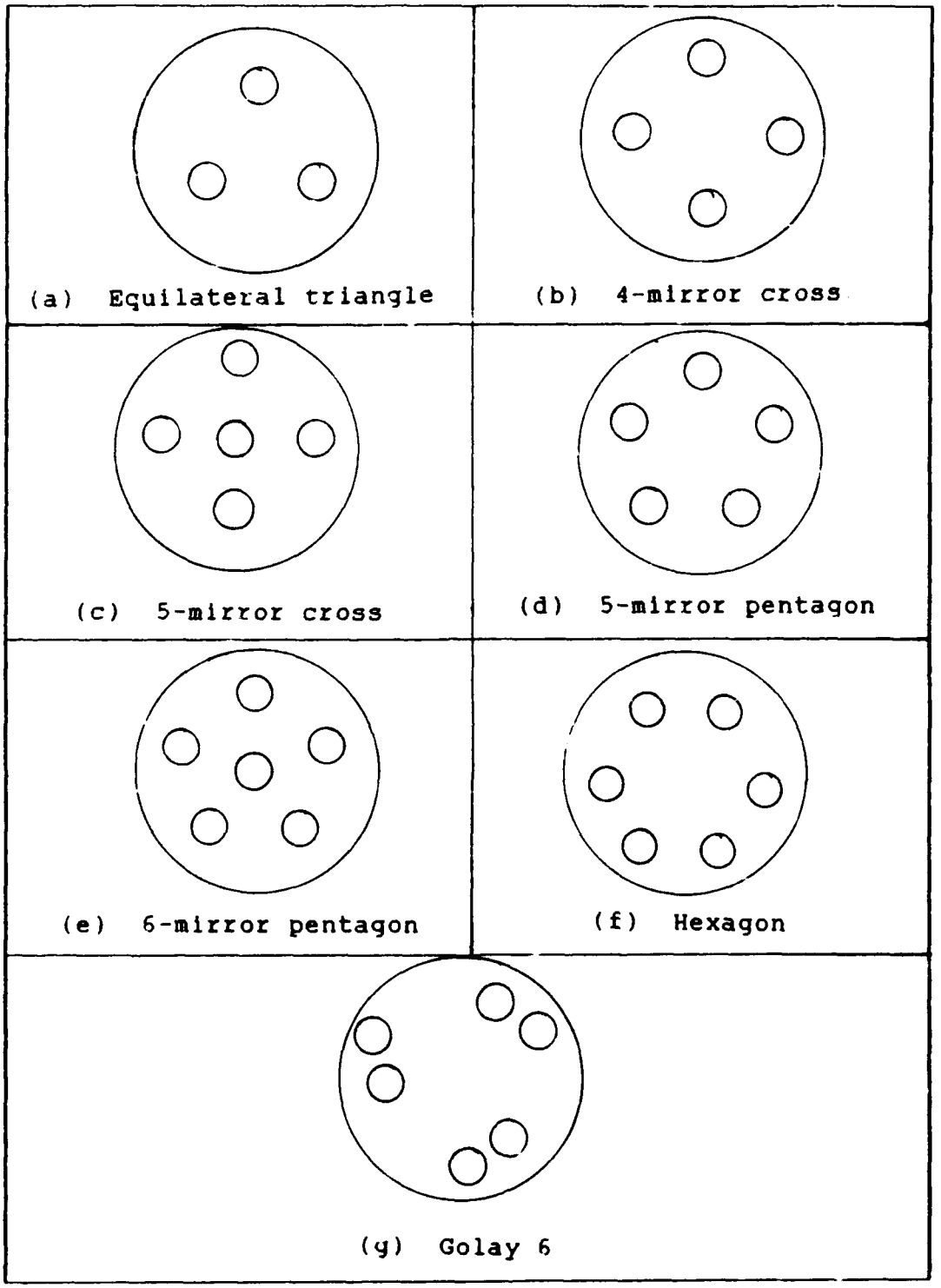

Figure 4. Mirror geometries

II. Theory

Introduction

This chapter lays out the theoretical background required in this thesis. The structure will be as complete as needed; however, it is by no means comprehensive. For a thorough background of Fourier optics, Gaskill provides an excellent and comprehensive discourse (9).

This chapter will cover the following areas: apertures and their various governing mathematical relationships, concepts used to model optical systems, Fourier transforms and how they enter into optics study, and finally, describe a different aspect of this thesis -- optimization of an aperture system.

Pupil Function

An aperture[1] can take on many possible shapes (square, round, hexagonal, etc.). Each shape has a unique mathematical function to represent that aperture's transmittance -- the way the light interacts when passing through the aperture. A square aperture is represented by a rectangle function; a circular aperture, the one this thesis studied, is represented by a cylinder function. In a single aperture, this single mathematical function represents the system's pupil function; in a multiple aperture system, a combination of each individual aperture's

[1] In this context, aperture refers to the shape of the primary optics used in the telescope system.

transmittance function determines the system's pupil function. This thesis is only concerned with circular apertures; the mathematical function used is the cylinder function.

The cylinder function is defined by (9:71)

$$\text{cyl}\left(\frac{r}{d}\right) = \begin{cases} 1, & 0 \leq r < \frac{d}{2} \\ \frac{1}{2}, & r = \frac{d}{2} \\ 0, & r > \frac{d}{2} \end{cases} \qquad (4)$$

d = diameter of the aperture

r = radius of the aperture

As seen from the equation, the cylinder function is equal to one as long as the radius is less than one-half the diameter of the cylinder; by convention, if the radius equals the diameter, the function's value is 1/2, and with the radius greater than half the diameter, the function's value is zero (Figure 5) (9:72). Physically, this function represents a circular pupil -- where the function equals one represents light passing through the pupil opening; where the function equals zero, the light hits outside the pupil and therefore the light does not pass through it.

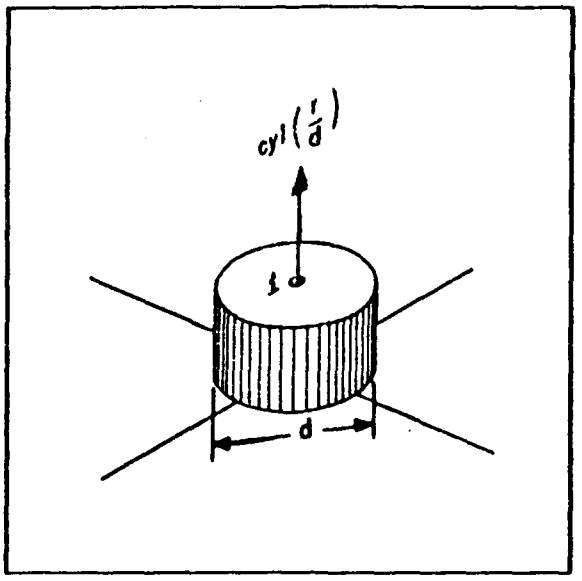

Reprinted from (9:72)

Figure 5. Cylinder function

Fourier Transforms and Optics

The Fourier transform is a powerful tool used in many aspects of physics and mathematics. As an example, using a Fourier series expansion, consider the rectangular wave function. Using a Fourier series, one can very closely approximate this function mathematically using sinusoidal waves (9:109). The more terms used in the series, the more closely the Fourier series will approximate the function. The function can now be manipulated in the frequency domain by multiplying the functions rather than performing complex and tedious convolution integrations; the original function, g(t), may be obtained by performing an inverse Fourier transform on the Fourier transformed function G(v), and the result will be the modification of the original

function in the time domain (9:180).

The Fourier integral decomposes the function g(t) into a linear combination of complex exponentials. If g(t) satisfies certain (Dirichlet) conditions, the function is described by the equation

$$g(t) = \int_{-\infty}^{\infty} G(\nu)\, e^{j2\pi\nu t}\, d\nu \qquad (5)$$

G(ν) is a weighting function and is called the Fourier transform of g(t); its value is given by the equation

$$G(\nu) = \int_{-\infty}^{\infty} g(\alpha)\, e^{-j2\pi\nu\alpha}\, d\alpha \qquad (6)$$

> The function G(ν) is also often called the <u>complex temporal-frequency spectrum</u>, or simply <u>frequency spectrum</u>, of g(t)... (I)t is a piecewise-continuous function of the frequency variable ν... (I)f all of these appropriately weighted components are added together in the proper fashion, the resulting function is just the original g(t), which is often referred to as the <u>inverse Fourier transform</u> of G(ν). (9:111-112)

G(ν) describes a Fourier transform in one dimension; ν is used to describe that frequency in inverse meters (m^{-1}); when working in two dimensions, the symbols ξ and η describe the spatial frequency components in the two directions. As in the one-dimensional case, ξ and η have the units of m^{-1}, and likewise can be used to reproduce two-dimensional shapes. An explanation of how this thesis graphically represents these two-dimensional spatial frequencies is in the next chapter.

Point Spread Function. For incoherent light, the point spread function of an optical system can be described as the

> ...system response to a point source of light in the object plane some distance away. In other words, it is the irradiance pattern that will result when this point source is imaged. Diffraction effects within any system will prevent the point source from being imaged back into another point. (16:15-16)

This point source of light (an impulse) is represented by a Dirac delta function (9:50). This function describes

> ...point sources, point masses, point charges, or any other quantities that are highly localized in some coordinate system....(I)f the system's impulse response is known, and if the system is a linear system we need only to decompose the complicated input into a superposition of a large number of delta functions, each appropriately weighted and positioned. The net response to the complicated input is then determined by adding together the responses to all of the individual delta functions. (9:50)

The output of a given system is the convolution of the system's point spread function with the scaled object on the image plane.

$$g(x,y) = f(mx,my) ** h(x,y) \qquad (7)$$

h(x,y) = point spread function

f(mx,my) = scaled object radiance

m = magnification

This may be regarded as "...a superposition of appropriately weighted and shifted impulse responses" (9:336).

However,

> ...it is usually quite difficult to calculate the output of a system by the direct evaluation of a convolution integral, and this difficulty is greatly magnified for two-dimensional systems. Consequently, except in special cases, the transfer-function approach is normally applied as a matter of course....(T)he output spectrum of...(this) system is given by

$$G(\xi,\eta) = F(\xi,\eta)H(\xi,\eta) \qquad (8)$$

(9:336-337).

To obtain the actual object image, one performs an inverse Fourier transform on the result $G(\xi, \eta)$.

Autocorrelation of the Cylinder Function. The cylinder function describes the circular aperture's pupil function; the autocorrelation of this function yields the Fourier transform of a circular aperture's point spread function. The rigorous derivation of the autocorrelation of the cylinder function is found in (9:303-305); Equation (9) yields the normalized cylinder-function cross correlation of two equal-size cylinder functions.

$$\gamma_{cyl}(r:1) = \frac{2}{\pi}[\cos^{-1}-r(1-r^2)^{\frac{1}{2}}]cyl(\frac{r}{2}) \qquad (9)$$

The variable r is a value depicting the difference between the centers' actual separation distance and their original separation; its value is derived in the next section. The Fourier representation of the point spread function is the Optical Transfer Function.

Optical Transfer Function and Modulation Transfer Function. To perfectly image an incoherent object, an optical system must be able to detect spatial frequencies from zero to infinity. This feat requires an aperture of infinite diameter. Anything less yields less than a perfect image of the object; as described by Equation (1), the larger the diameter of the system, the better the image resolution (at a given wavelength). One can now describe the capability of the system by the maximum spatial frequency the system can detect. This determines the resolution limit of the system in the spatial domain. The Fourier transform of the point spread function is known as the Optical Transfer Function (OTF). A rigorous derivation of the OTF is found in (9:493-497). The result is

$$H_{2S}(\xi,\eta) = \frac{[p_4(x,y) \star\star p_4^*(x,y)]^*|_{x-\lambda z\xi/m,\, y-\lambda z\eta/m}}{\text{area of aperture stop}} \qquad (10)$$

However, for a single circular aperture,

$$p(x,y) = cyl(r) \qquad (11)$$

so the numerator of Eq (10) becomes

$$\begin{aligned} p_4(r) \star\star p_4^*(r) &= cyl(\tfrac{r}{d}) \star\star cyl^*(\tfrac{r}{d}) \\ &= \frac{\pi d^2}{4}\, \gamma_{cyl}\,(\tfrac{r}{d}:1) \end{aligned} \qquad (12)$$

Eq (12) equals the normalized cylinder function cross-correlation.

In solving for the value r to be used in Eq (9), one must transform the rectangular coordinates into polar coordinates; mathematically, r represents the actual distance between aperture centers plus or minus the original distance between centers. But since we are in frequency space, the x and y values are dummy variables; their actual values are (9:494)

$$x = \lambda f \xi \tag{13}$$

$$y = \lambda f \eta \tag{14}$$

where

x = rectangular coordinate of aperture

y = rectangular coordinate of aperture

f = focal length

ξ = spatial frequency

η = spatial frequency

In a one-aperture pupil, the original distance between centers is zero and so the value for r is (9:494)

$$r = \sqrt{(\frac{\lambda f \xi}{d})^2 + (\frac{\lambda f \eta}{d})^2} \tag{15}$$

so one obtains the value of r at the spatial frequencies ξ and η. The resulting value of r is then plugged into Eq (9). The value obtained by Eq (9) gives the magnitude of

the OTF at the chosen spatial frequencies ξ and η ; the value of this function is greatest at r = 0, and goes to zero when r = 1; the purpose of the cylinder function at the end of Eq (9) is to force the value of the function to zero when r = d. This function is evaluated at all desired values of ξ and η to obtain a three-dimensional spatial representation of the pupil's OTF (9:495).

To evaluate a pupil function with two apertures, one performs the autocorrelation on each individual aperture, then a cross-correlation of the pair of mirrors. Eq (12) becomes

$$\begin{aligned} p \star\star p = {} & 2\gamma_{cyl}\left(\frac{\lambda f\xi}{d}, \frac{\lambda f\eta}{d} ; 1\right) \\ & + \gamma_{cyl}\left(\frac{\lambda f\xi - a}{d} , \frac{\lambda f\eta - b}{d}\right) \\ & + \gamma_{cyl}\left(\frac{\lambda f\xi + a}{d} , \frac{\lambda f\eta + b}{d}\right) \end{aligned} \tag{16}$$

Eq (15) becomes

$$r = \sqrt{\left(\frac{\lambda f\xi - a}{d}\right)^2 + \left(\frac{\lambda f\eta - b}{d}\right)^2} \tag{17}$$

a = Δ x between aperture centers

b = Δ y between aperture centers

In the two mirror example, with mirror centers on the x-axis, b = 0. To obtain the OTF of a system of three or more mirrors, one performs an autocorrelation on the three-mirror pupil. In deriving this transfer function and in all subsequent calculations of transfer functions in the thesis,

the values of d (diameter) and f (focal length) were set to one meter.

The OTF takes into account all aspects of the system to include system aberrations and other imperfections such as atmospheric distortion; if one considers a perfect system (as this thesis does), there are no phase shifts, and one can simplify the OTF by considering only its modulus, or Modulation Transfer Function (MTF) (9:497), as described in chapter 1.

Determining Significance of Increase in Resolution

The best way to determine the significance of any increase in resolution is to quantitatively study the difference in the output of the mirror system between the single wavelength optimum and its corresponding multiple wavelength optimum. The scope of this thesis did not allow for such a comprehensive study; however, a program was set up to qualitatively determine whether the increase in resolution was detectable and significant. This section details the derivation of the equations used in the computer routine.

The Thin Lens Law is used as a starting point.

$$\frac{1}{o} + \frac{1}{i} = \frac{1}{f} \tag{18}$$

where o is the distance from the lens to the object, i is the distance from the lens to the image, and f is the focal length as illustrated in Figure 6.

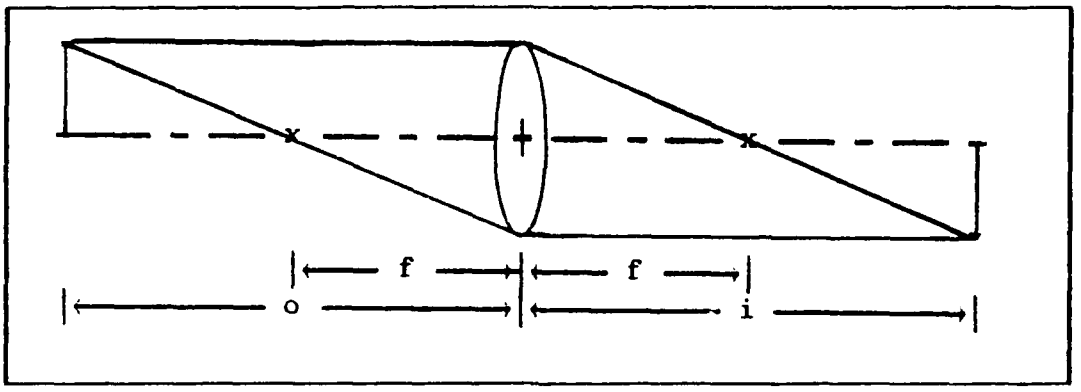

Reprinted from (16:13)

Figure 6. Simple thin lens imaging

Magnification is defined as (1:269)

$$\text{linear magnification} = \frac{\text{image distance from lens}}{\text{objectdistance from lens}} \tag{19}$$

or

$$m = \frac{i}{o} \tag{20}$$

If the object distance is sufficiently large, the equation simplifies to

$$m = \frac{f}{o} \tag{21}$$

In this thesis, f = 1, so the equation becomes

$$m = \frac{1}{o} \tag{22}$$

or, magnification is the inverse of the object distance from the pupil. This is the scaling factor is used in Equation (7).

The output of a system is the inverse Fourier transform of Equation (8). The function $H(\xi, \eta)$ is the MTF of the pupil; the function $F(\xi, \eta)$ is the scaled transform of the object under observation. In this case, the object is a sphere, but at a great distance the sphere appears as a two-dimensional disk, its shape defined by the cylinder function (Fig.5). The Fourier Transform of the cylinder function is the sombrero function (9:329). Scaling the sombrero function by the magnification and multiplying the scaled function by the MTF yields the Fourier representation of the object as detected by the system. When performing the inverse transform on $G(\xi, \eta)$, one should obtain the original cylinder function. But, since the object is at a great distance from the pupil, there will be degradation of the cylinder function, evidenced by the rounding off and smoothing out of the cylinder. The limit would be imaging a coherent point source, its inverse transform being $g(x,y) = 1$. By comparing the relative rounding off with the sphere at a distance near the resolving limit of the mirror system, one can qualitatively determine if the resolution has increased between the single wavelength system and the multiple wavelength system.

Optimization

The field of Operations Research specializes in many techniques and algorithms for optimization. The thesis takes advantage of one such routine in an attempt to optimize mirror configurations utilizing Harvey's criterion

for determining mirror system diameter. A function, called an objective function, is developed to describe with one variable the value to be optimized. In this case, the objective function is defined as the maximum spatial frequency value at which the first zero appears in a system's MTF. This objective function is maximized using a modification of the Hook and Jeeves optimization algorithm (14:511).

The original Hook and Jeeves algorithm operates as follows (this explanation will be for a maximization problem in a Cartesian coordinate system). A start point is chosen. From this base point, one moves a distance plus and minus ε (epsilon) in the x direction from the point. The function is evaluated at these points, and the best objective function point is chosen as the temporary point. From this temporary point, the function is evaluated plus and minus ε in the y-direction. Again the function is evaluated and the best point chosen. If the temporary point is any point other than the original base point, a base 2 is set up at point 2 * ε in both the x and/or y direction from the original base point. This new base is the start of the next exploratory search. This search continues until there is no change in the temporary base; the latest temporary base becomes the new permanent base. The ε is cut in half, and the search begins at the new base point. This move and evaluate, find a new base and cut ε continues until ε reaches a predetermined value. At this point, the search

ends and theoretically, the function has reached its maximum within the errors of the chosen minimum ε (14:511-515).

The Hook and Jeeves method is a powerful method of finding the optimum value of a function, especially if the function does not lend itself to differentiation, a basis for many other optimization routines (13). The method has its disadvantages, however. The method works best on smooth, continuous functions with no discontinuities. Another major drawback is that it does not differentiate between local minima (maxima) and global minima (maxima). This may cause the algorithm to choose the wrong optimum point; in this case, the algorithm is sensitive to starting point. A possible solution to this problem would be to run the algorithm using random start points. This does not guarantee finding the global optimum, but increases the chances of finding it.

The multiple aperture system is much more complex than the simple single function optimization routine. In this case, there are from two to six (or more) apertures that are interrelated. The relative movement of the mirrors has a critical effect on the objective function value; the decision to move one mirror at a time or several at once before evaluating the function will cause the final aperture position to vary. The next chapter will describe the method used to move the mirror system.

III. Methodology

Introduction

This chapter will cover the practical application of the theoretical foundation laid out in the previous chapter. Specifically, it will describe how to interpret the three-dimensional and contour representations of the MTF, it will cover the formulation of the various computer codes used in the thesis, the specific ways the code was used to generate the data needed to accomplish the desired goals, and will conclude with a detailed explanation of the optimization algorithm used to optimize the results using Operations Research methods. Wherever applicable, the explanations will use the four mirror cross (Figure 1b) as a basis for examples.

Graphical Representation of the MTF

As previously discussed, the MTF represents sinusoids directed over 360^0. These sinusoids are decomposed into their ξ and η components.

> ...The temporal frequency of a time-varying sine wave describes the number of oscillations made by the function per unit time; for a function that varies sinusoidally with some spatial coordinate, the spatial frequency associated with the function in that same direction indicates the number of repetitions the function makes per unit distance. (9:129)

The two primary methods this thesis uses to graphically represent a pupil's MTF are the three-dimensional plot and the contour plot (Figure 7).

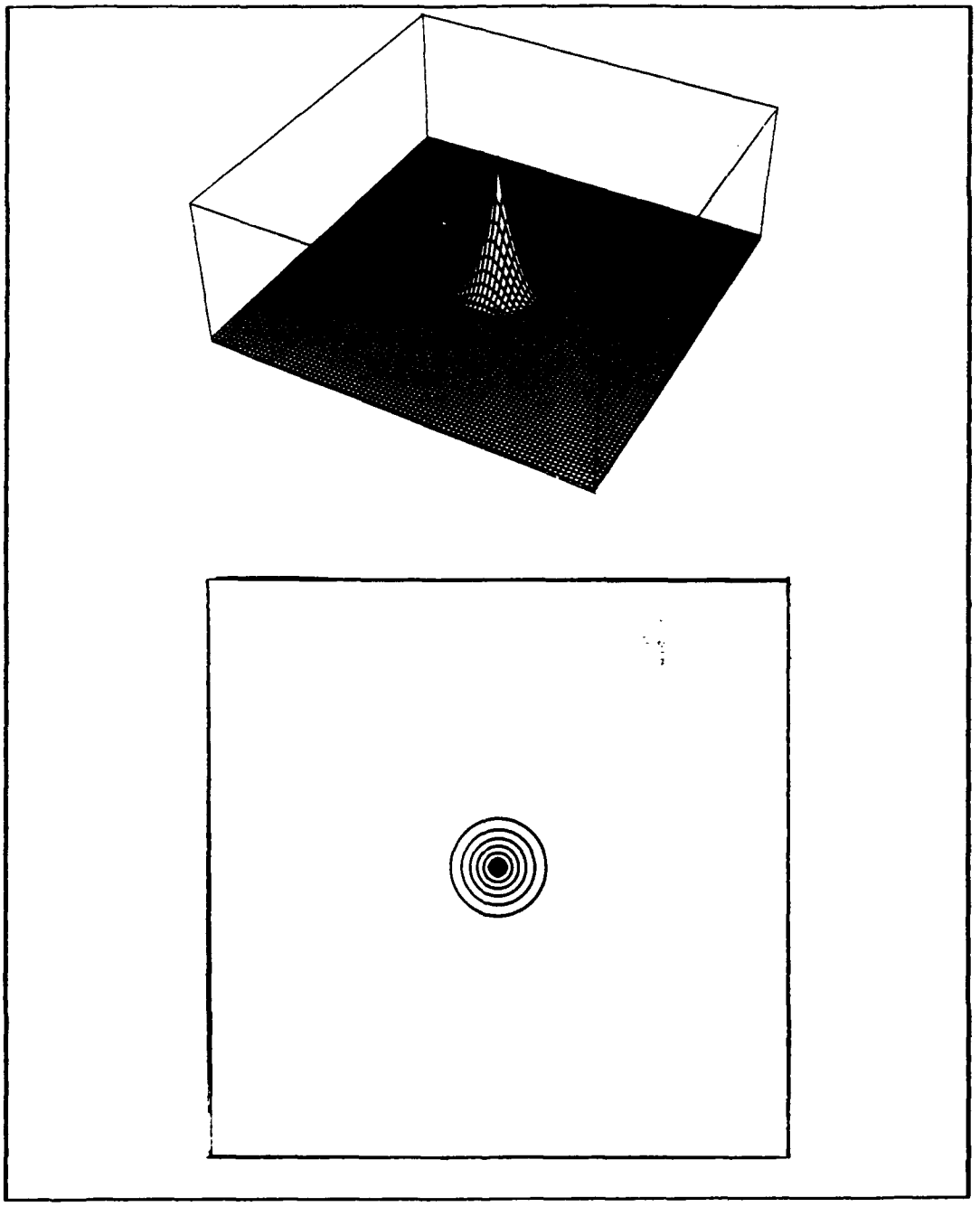

Figure 7. MTF of a one mirror system

There is no scale depicted with either representation; it varied depending on the number of mirrors in the system as well as mirror spacing. However, unless otherwise specified, the maximum spatial frequency used was 1.5×10^{5} m^{-1}; this corresponds to the outer edge of the plot box in the contour plot and the edge of the grid in the 3-dimensional plot. In examining the three-dimensional plot of the single mirror pupil at three microns (Figure 7a), the peak corresponds to DC -- zero cycles per meter. At this point, the value of r in Equation (17) equals zero. Since the MTF is normalized, the value at this zero point is one. The MTF plot then slopes symmetrically in all directions down to zero, corresponding to the maximum spatial frequency the pupil can detect. The corresponding value of r is one. For a single mirror, one meter diameter pupil at three microns, this equates to a maximum spatial frequency value of 3.33×10^{5} m^{-1} (Figure 7). The change in spatial frequency from one side of the cone to the other at its base is 6.66×10^{5} m^{-1}. In a multiple mirror system, since each mirror is autocorrelated, each gathers information as if it was an independent mirror; therefore, the peak value of the MTF at the center of the plot (the tip of the peak corresponding to zero) is equal to the number of mirrors in the system (prior to normalization). Figure 8 shows the MTF of a four-mirror pupil; prior to normalization, the central peak value is four. The point at which the central cone reaches zero has a spatial frequency

value of 3.33×10^5 m^{-1}. The value of the MTF corresponding to the cross-correlated mirrors are to the outside of the central peak; this graphically depicts the system's ability to detect higher spatial frequencies. At three microns, each of these outer cones has a spatial frequency difference of 6.666×10^5 m^{-1} across the base.

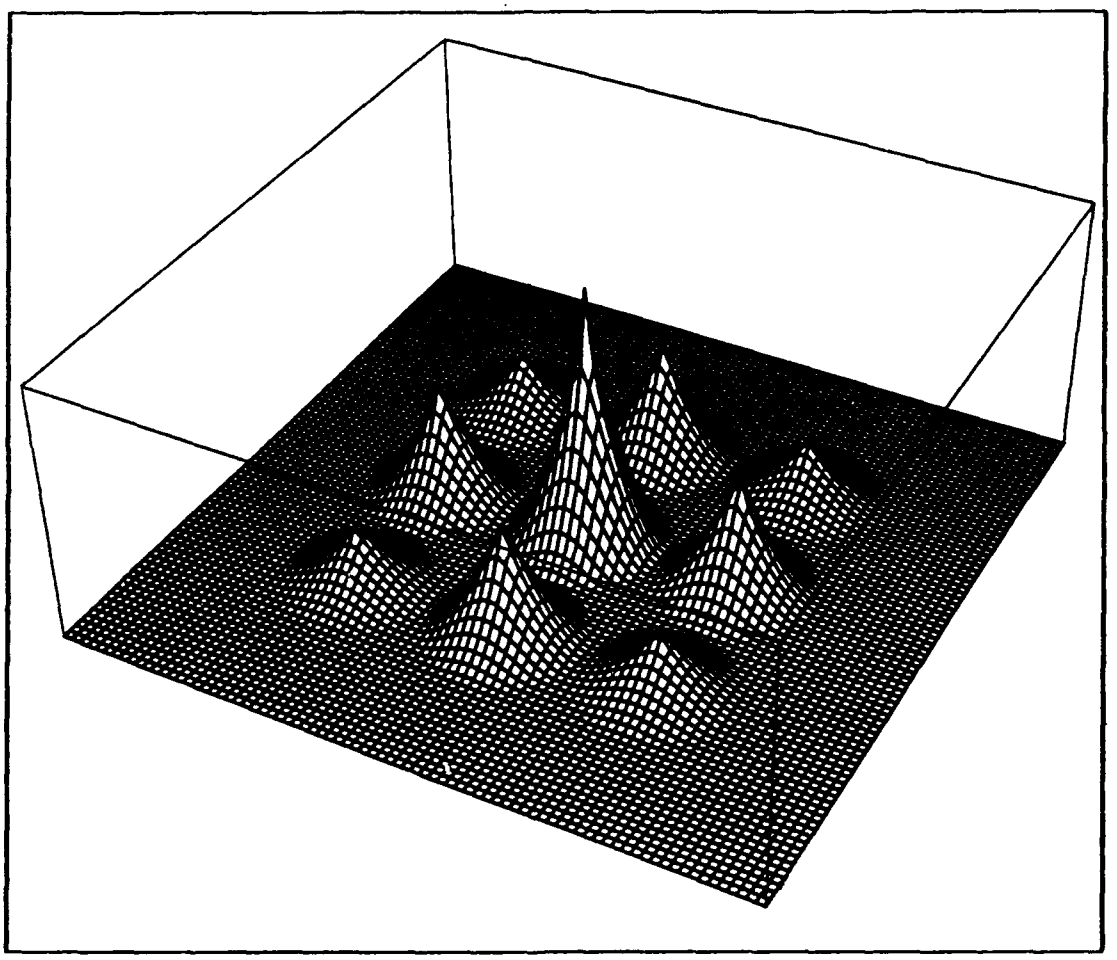

Figure 8. Four Mirror MTF plot

The plot changes as the detection wavelength increases. Figures 9 and 10 show the four-mirror cross MTF at three and five microns with the mirror spacing remaining constant. The three micron MTF cones have the dimensions as described above, but the five micron MTF cones now show the decrease in the system's detection ability. The entire MTF pattern has shifted inward, and the spatial frequency shift at the base of each cone is now only $2.0 \times 10^{5}\ m^{-1}$. The entire geometry of the MTF pattern -- the spacing between the cones as well as the spatial frequency difference along the base -- has decreased by three-fifths. This, again, corresponds to Equation (1) -- as the wavelength increases, the maximum resolution proportionally decreases. This thesis takes advantage of this inward shift at longer wavelengths to fill in the interior gap at a single wavelength caused when moving the mirrors outward.

The three-dimensional plot nicely shows the magnitude of the system, but a much more useful qualitative representation of the MTF is the contour plot. With this plot, one can get a clear idea of what is happening as the mirrors of a multiple mirror system move in or out (Figure 11). As each mirror system was studied at the single, three micron wavelength, its corresponding contour plot displayed the MTF system expanding, and, as the mirrors were moved out, one could predict where the MTF pattern would separate, thus determining the maximum distance allowable in the

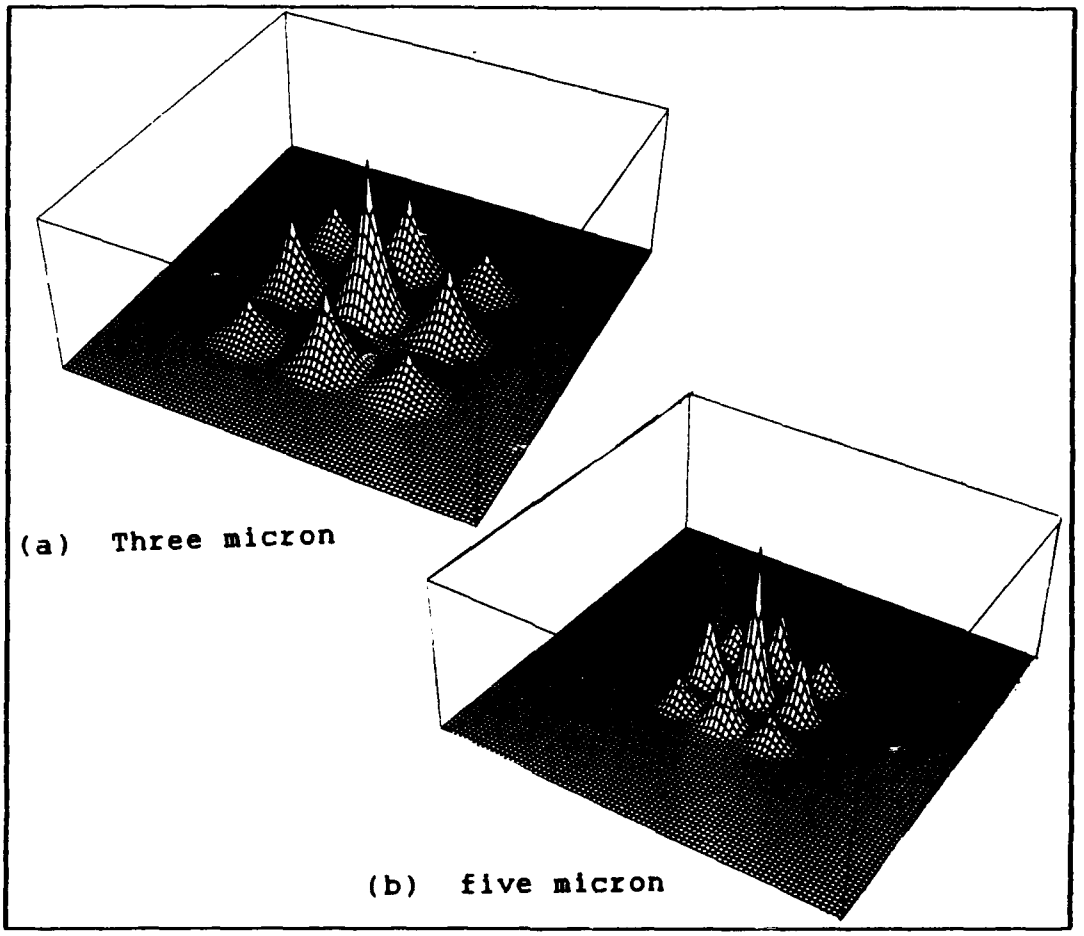

Figure 9. Three- and five-micron 3-dimensional plots

mirror system (Figure 12). The contour plots were also useful in predicting whether the use of multiple wavelengths would allow for an increase in the spacing of the mirrors, thereby increasing the maximum possible spatial frequency of the system and its maximum possible resolution. As with the three-dimensional plots, the contour plots were used only to visualize the configuration of the MTF. "The contour lines correspond to an evenly-spaced sequence of z values" (21:135).

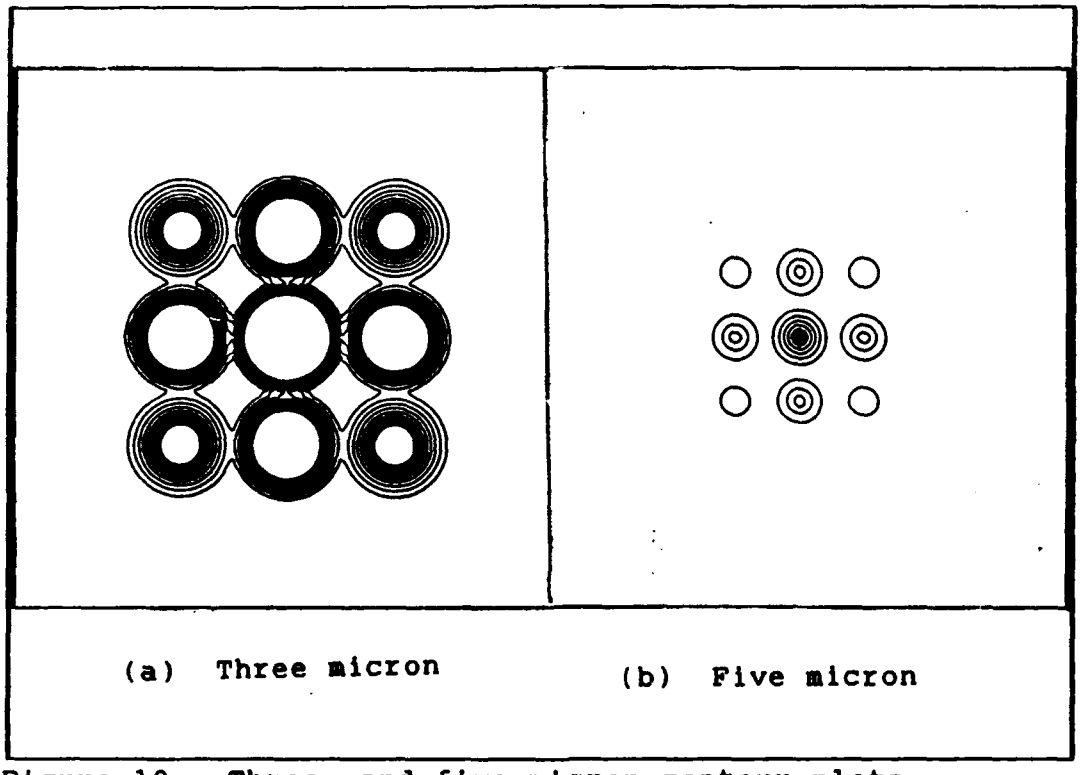

Figure 10. Three- and five-micron contour plots

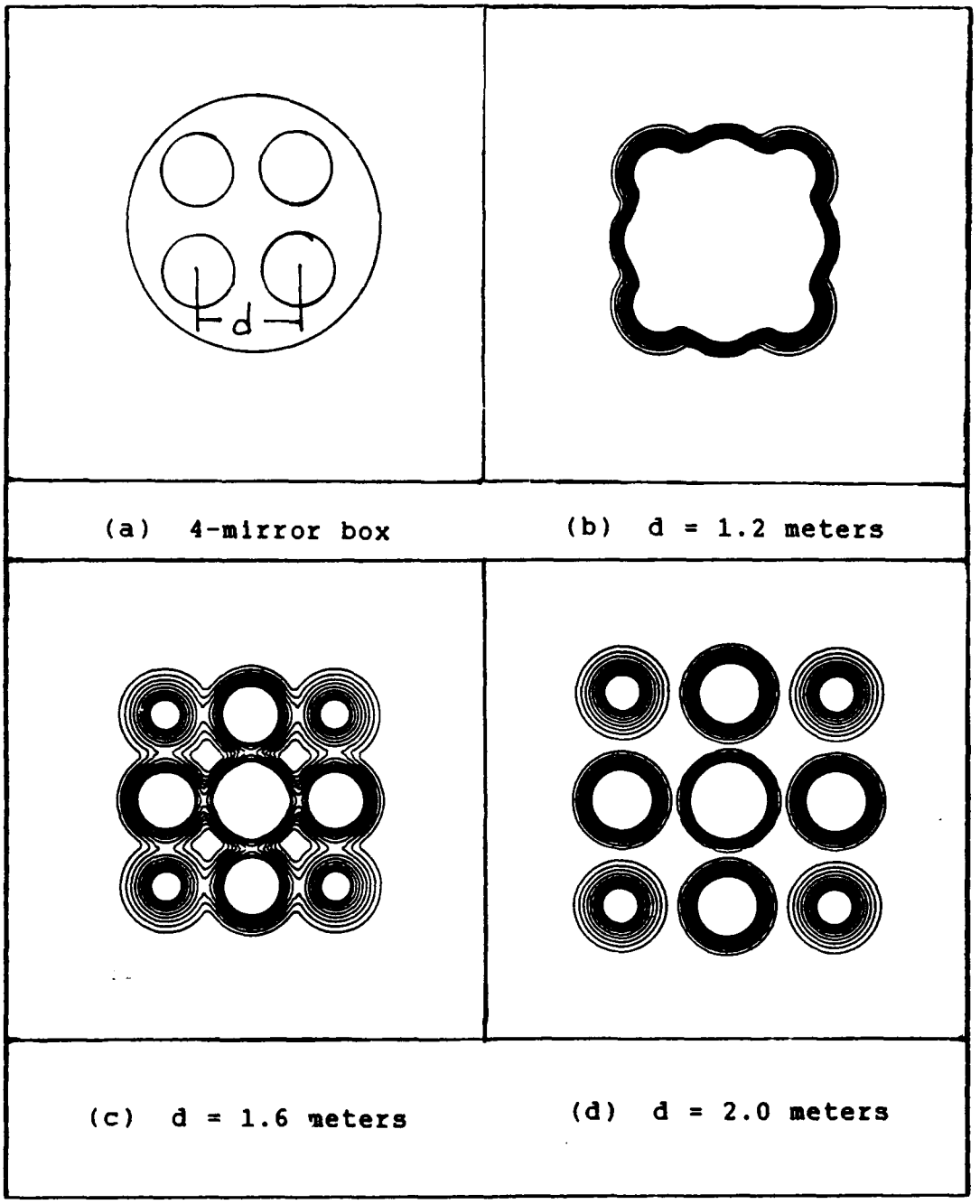

Figure 11. Contour plots of four mirror pupil at various mirror distances

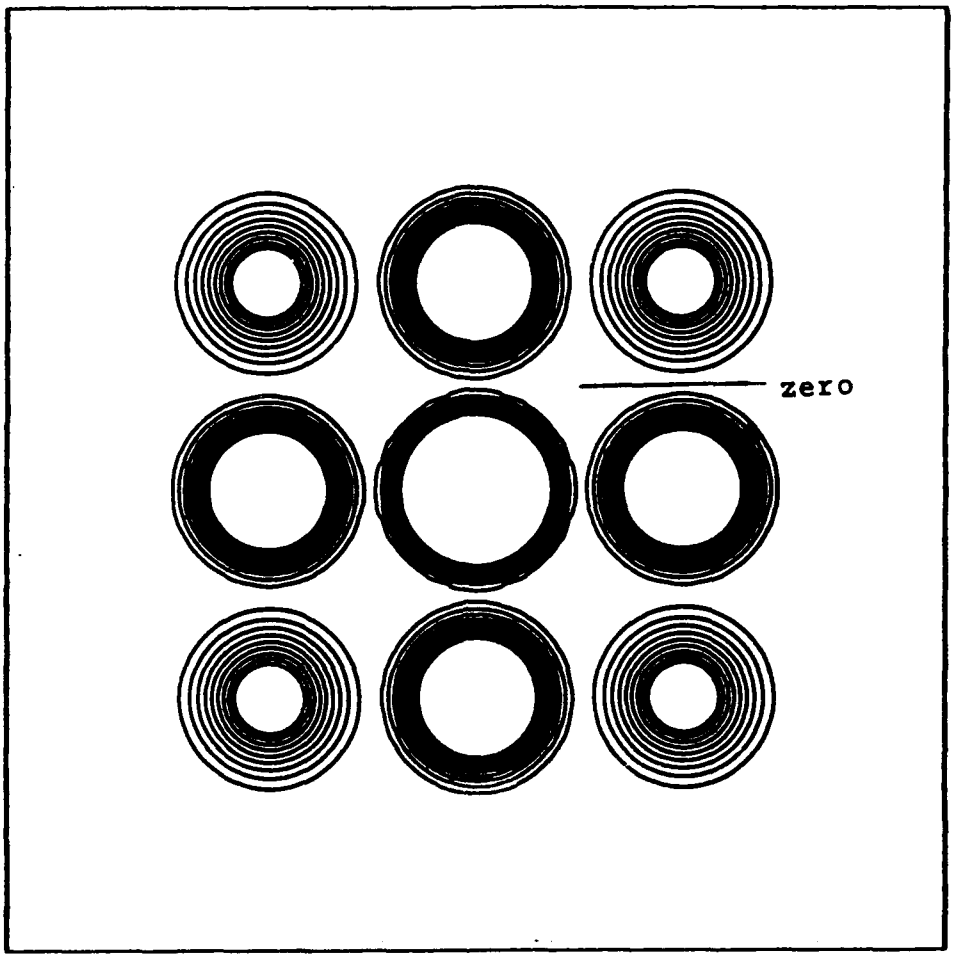

Figure 12. Contour plot showing interior zero

Computer Routines

All of the computer programs were written in Fortran. They were compiled and executed using Fortran 77 on an ELXSI 6400 mainframe computer. The main code used in generating the MTF array is found in Appendix A. There were many variations of this code modified to specific needs, such as varying the array size to allow for clear graphics and

expanding of one quadrant of the matrix to more exactly determine when the mirror system was spread too much, causing the first zero to occur close to the center (Figure 12). One code, written to evaluate the significance of the increased resolution, requires the mathematical subroutine library, IMSL, version 9.2. To allow for ease in loading in initial values, a code was written to enter the initial values into a file. The main code then took the values from this file (see Appendix B). The optimization routine will be covered later in the chapter.

The main computer routine performed its task in two parts. The first portion of the program generated the MTF array based on the initial conditions. The second part of the program performed a search of the array to determine the minimum MTF. This value, as well as the spatial components at which the minimum zero occurred was then written into an output file.

Determining Optimum Configuration

In this thesis, the bandwidth used was from three to five microns. Any small wavelength range could be used; with scaling, the results of this thesis can be applied to any wavelength range. The three-to-five micron range was chosen as a representative bandwidth because this range represents an atmospheric "window" through which one can survey the Earth's surface (4); current research is expanding research and development of sensors at this wavelength spectrum (12:57).

Spectral information can be gathered in two ways: the first is by using a broadband sensor to detect all the frequencies throughout the chosen wavelength spectrum; the second is by splitting the incoming light into several parts, each part going to a discreet, single wavelength, sensor. The techniques are different, but this thesis considered the received information past the sensors; the computer model approximated the broadband detection by simply decreasing the step size when going from one end of the wavelength spectrum to the other. In practice, the half-micron step size used in the computer runs adequately modeled either configuration.

Once a pupil configuration was chosen, computer runs were made at the three micron wavelength to determine the maximum attainable MTF. The three micron wavelength was chosen as the baseline, reasoning that, if the system was to use only one wavelength, the one yielding the first zero occurrence furthest from the origin would be the logical choice. Figure 13 graphically depicts the slow increase in the minimum zero MTF occurrence up to the point where a gap develops in the interior of the system, causing an abrupt drop in the minimum MTF value. In this graph, the x-axis is the radius of a circle which would enclose the mirror system.

Once the optimum mirror spacing was determined for the single wavelength, the three to five micron wavelength band

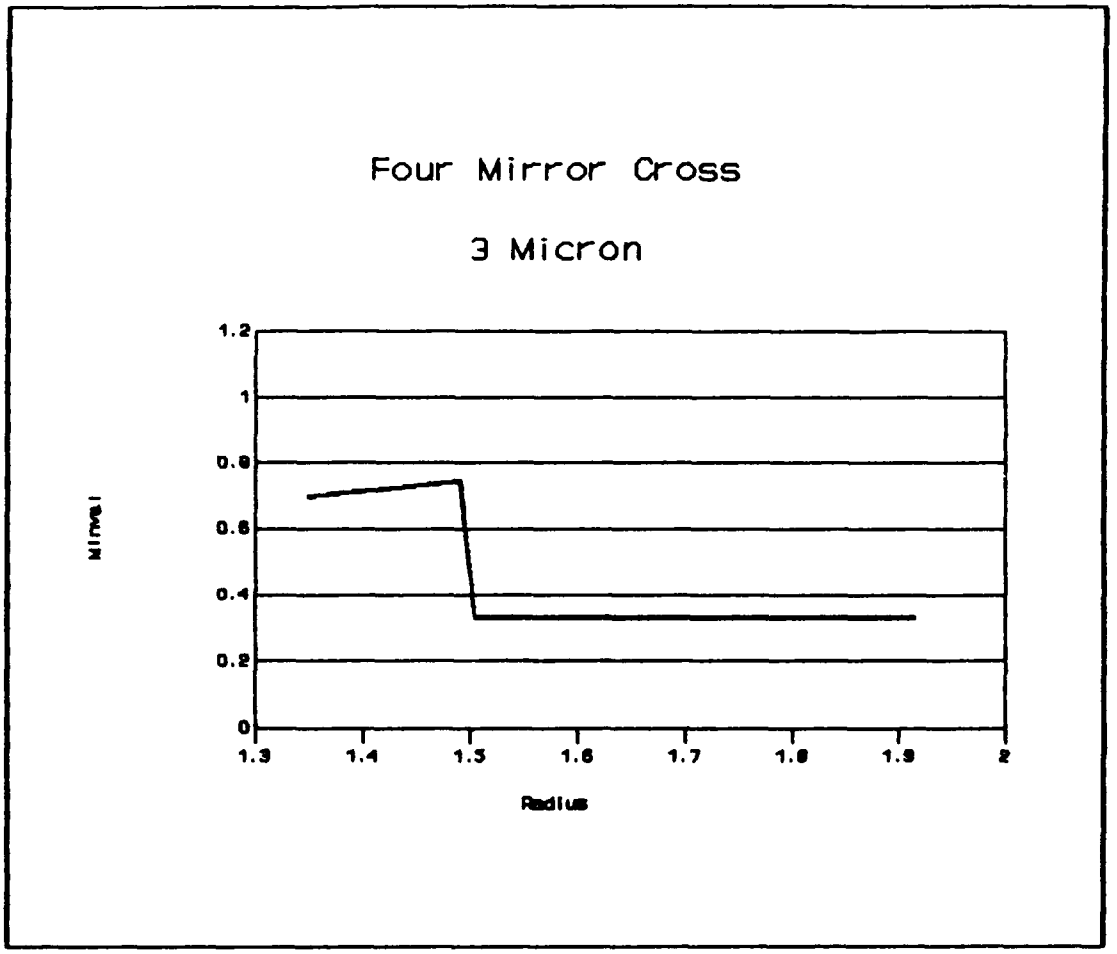

Figure 13. MTF as radius increases

was tested to see if the MTF from the other wavelengths could be used to fill in the interior zero created by increasing the spacing between the mirrors. Mathematically, this was accomplished by computing the system's MTF at intervals of one-half micron from three to five microns. The results were stored in a single array. Graphically, this showed how the various wavelengths contributed in filling in the interior of the MTF, thus allowing the size of the mirror system to increase, increasing its spatial resolution

(Figure 14). In the four mirror case, the use of the broadband wavelength spectrum allowed for an 8.3% increase in the MTF (from 7.44 x 10^5 m^{-1} to 8.06 x 10^5 m^{-1}).

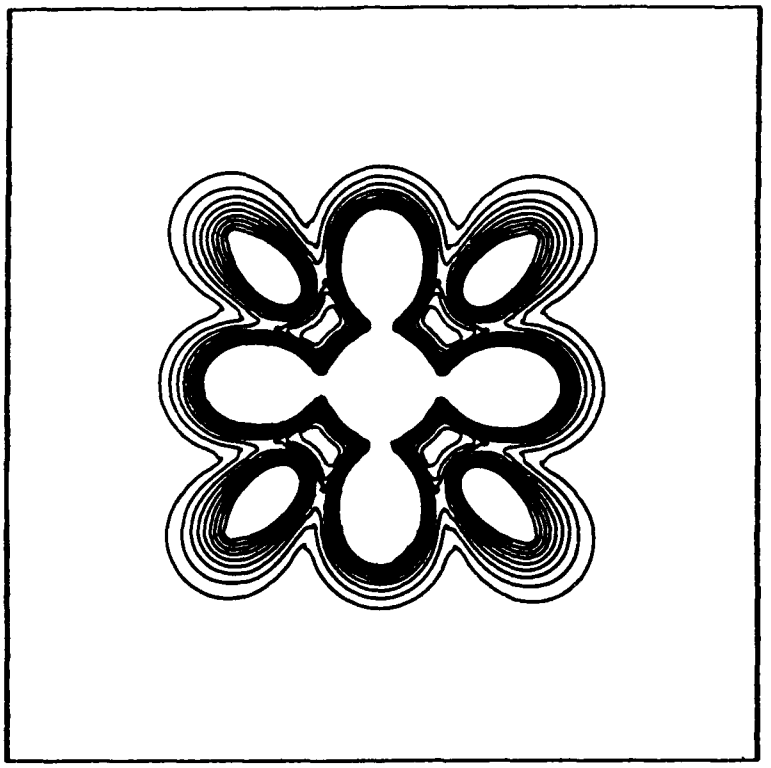

Figure 14. MTF of optimum four mirror cross at three to five microns wavelength

Comparison of Mirror Systems

Using Harvey's criterion for determining the maximum frequency before reaching a zero MTF value yielded a very straightforward method for directly comparing any mirror system. The thesis also uses this maximum MTF value to

compute the single mirror equivalent. This single mirror equivalent value is used to compare the various mirror systems in the results.

As stated earlier, in a single mirror system, the MTF value goes to zero at the point where the value r in Equation (17) equals one. Setting $r = 1$ and solving at a point where $\eta = 0$ yields

$$1 = \sqrt{(\frac{\lambda f \xi}{d})^2} \tag{23}$$

or,

$$d = \lambda f \xi \tag{24}$$

However, with the focal length value f set to one, the equivalent single mirror diameter is

$$d = \lambda \xi \tag{25}$$

This equivalent single-mirror diameter (in meters), solved at a wavelength of three microns, is a very effective method of comparing the various multiple-mirror counterparts.

Determining Resolution Increase Significance

As described in chapter two, the sombrero function describes the Fourier Transform of the cylinder function. Instead of generating a cylinder function and taking its transform, a simpler method of incorporating the function is

to generate the appropriate sombrero function, properly scaled by the desired distance from the pupil. This was accomplished using the following (9:72,329):

$$\frac{\pi}{4}\,\mathrm{somb}\left(\frac{\rho}{d}\right) = \frac{\pi}{4}\left\{\frac{2J_1\left(\frac{m\pi r}{d}\right)}{\left(\frac{m\,\pi\,r}{d}\right)}\right\} \qquad (26)$$

rho = spatial frequency

m = magnification (inverse distance as given in Eq 22)

d = diameter (1 meter)

J_1 = first-order Bessel function of the first kind

The resulting array is then multiplied by the appropriate MTF. The inverse transform of this array yields the cylinder function, or, since the object is far away, it yields the degraded *cylinder function*. Taking a cross-section of this cylinder, one can use the slope to determine the relative system degradation and use this slope to compare various systems -- the steeper the slope, the better the system resolved the object.

Optimization

As stated in the previous chapter, a modified Hook and Jeeves algorithm was used in the search for optimum mirror configurations. The program, listed in Appendix C, has two distinct modifications to the original algorithm.

The first modification was in the way the mirror positions were tracked. Instead of using Cartesian coordinates, polar coordinates were used. This allowed for

a unique method of linking the mirrors in the system. the first mirror was anchored to the origin; it never moved. The second mirror was defined as a radial distance from the first mirror and could only move along the x axis. The third mirror was defined at a radial distance and angle from the second mirror, the fourth mirror was defined as a radial distance and angle from the third mirror, and so on. This allowed for a more robust search for an optimum value. Whenever the second mirror moves, all the subsequent mirrors move in the Cartesian coordinate system; however, their relative position in the polar coordinate system remain constant. This allows for a much easier tracking of the entire mirror system.

The second major modification to the basic algorithm was not using temporary points and not moving a distance of 2 * ε when an optimum point was found in a given direction. The use of the 2 * ε jump is primarily designed for the search of an optimum in a smooth function; moving in such a way in this application would have opened the possibility of moving into a region where the MTF value suddenly decreased (the mirrors moved apart sufficiently to allow for a zero component much nearer the origin); there would possibly be no way to recover from such a jump. The decision was made to allow for a slower, more methodical search.

The search pattern proceeds as follows (using the four-mirror system as the example). The first mirror is anchored to the origin. From an initial set of polar coordinates,

the second mirror moves a distance ε in the plus radial direction. The complete mirror configuration is transformed into the Cartesian coordinate system (mirrors three and four move along with mirror two). The resulting coordinates are used to generate an MTF array and the array is evaluated to determine if the minimum MTF of the system has increased. If it has, the new mirror coordinates are kept. If not, the second mirror moves ε in the minus radial direction. Again the system is transformed into the Cartesian system and evaluated. Again, if the resulting spatial value increases, the new mirror positions become the starting point of the next phase of the search. The second mirror does not move in the theta direction, so after this set of moves (or attempted moves), the search moves on to the third mirror. A move of the third mirror only affects the fourth mirror. The third and fourth mirrors are evaluated in both the r and theta direction. When the fourth mirror evaluation is complete, the computer routine checks whether any of the mirrors have moved. If yes, the mirrors are evaluated again at the same ε, if no, the step size is halved and the system is evaluated at the new ε. This continues until the routine reaches a predetermined ε; the routine ends and, hopefully, a global optimum value is obtained.

As stated earlier, this algorithm is not able to determine whether the optimum attained is a local or global optimum; several runs were performed with each mirror

number using various initial mirror positions as well as changing the initial ε in both the r and theta direction in an attempt to attain the global optimum.

IV. Results

Introduction

This chapter is divided into three sections: the first section contains a discussion of general observations made throughout the thesis effort. The second section contains the actual numerical results for each mirror configuration studied. Each mirror configuration is discussed, the single and multiple wavelength equivalent diameters are analyzed and compared, and, if there was an optimization run performed using that mirror configuration, the symmetrical and the Operations Research determined optima are compared. The final section contains the results of the qualitative comparison of the resolving capability of the Golay six mirror configuration.

The term "ring", used throughout this chapter, is used to describe each single MTF contour that forms when the cones in the three-dimensional representation of the MTF are mapped onto a contour representation of the overall MTF (Figure 7). These rings often blend together, especially when the mirrors are close together or a broadband contour plot is analyzed (Figures 24 and 26).

General Observations

Observing the changes in the MTF of a particular system when going from a short wavelength (three microns) to the long wavelength (five microns), one notes that as the wavelength increases, the outer rings contract radially

towards the central ring; the rings also decrease in diameter (as described in chapter three).

As the spacing of each particular mirror configuration was expanded to obtain the optimum MTF for that configuration, the point at which the MTF opened up to allow an interior zero was always at the edge of the central ring and between two rings of the next outer series that formed a symmetrical arrangement about the central ring (Figure 17). This result was significant; because the interior zero always occurred at this point, some mirror configurations would not improve when including the MTF from longer wavelengths.

Odd Mirror Symmetrical Systems. For both the three-mirror and five-mirror symmetrical systems (triangle and pentagon), there was no improvement in the MTF from the single, three-micron to the broadband three to five micron wavelengths. On studying the plots of these systems (Figure 17 and 28), one observes that the outer rings form a symmetrical pattern equidistant from the central ring. The place at which the single wavelength MTF incurs its interior zero is as described in the previous section (Figure 17). As the wavelength increases, the rings radially contract toward the center (as expected), but, because of this equidistant arrangement, there is no benefit derived from the use of the multiple wavelength MTF because the rings are contracting at the same rate as they move inward. The MTF information from the longer wavelengths is not able to fill

in the gap at the center ring where the MTF originally opens up. Another way of looking at this phenomenon is -- if one can draw a line from the origin and not intersect any ring in the MTF pattern at a single wavelength, there can be no improvement in the MTF using a multiple wavelength MTF scheme (Figure 17 and 28).

Golay Configurations. The Golay patterns and their resulting MTF patterns were studied in Golay's paper (10:272,273). The patterns were attractive at first because the idea was to have no redundancy in the autocorrelations (no overlap of the rings). However, the Golay patterns used strictly the non-redundancy criterion in determining the mirror configurations; although more spatial frequencies can be detected, the first zero in many of the systems occurred close to the center, as seen in the four-mirror Golay pattern (Figure 15). The only mirror configuration that was of benefit to this thesis was the Golay-six pattern. This configuration is a nonredundant system; its MTF is highly symmetrical, thus allowing for a high minimum MTF value when evaluated using the thesis criterion.

Operations Research Optimizations. The optimization routine yielded surprising results. The original assumption was that the optimum patterns would yield symmetrical mirror configurations, so much of the thesis effort was devoted to

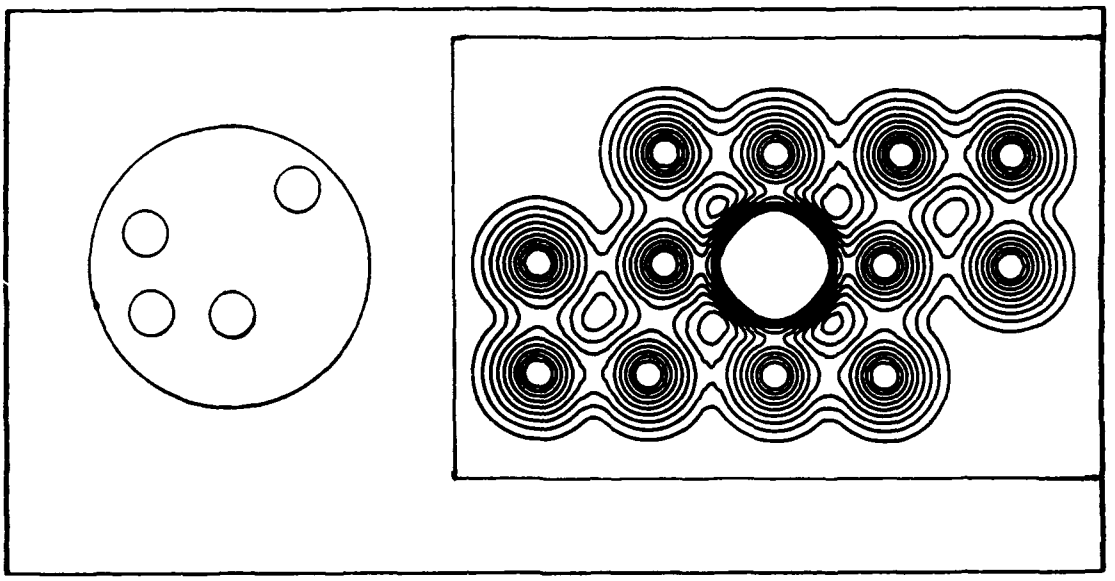

Figure 15. Four-mirror Golay

optimizing the symmetrical configurations. The results from the OR routine gave non-symmetrical mirror configurations and significantly higher MTF values than their symmetrical counterparts. As stated previously, these results may not be global optima, but in general are much better results than were obtained using trial and error with the symmetrical systems.

Detailed Results

This section contains the results obtained from all of the mirror configurations studied. Each section will describe the particular configuration, give the single-mirror equivalent diameter (E.D.) optimum value, the three-to-five micron single-mirror equivalent diameter optimum value, the percent resolution increase (if any) obtained going from single to multiple wavelength, and finally,

compare the results from the OR optimization of the particular system with its symmetrical counterpart. The mirror configurations are not necessarily to scale; Appendix D contains the actual xy coordinates of all the systems studied.

Three-Mirror Equilateral Triangle. As discussed in the previous section, the three-mirror equilateral triangle did not benefit from the multiple wavelength scheme because its outer rings were equidistant from the central ring. The OR optimization obtained the identical equilateral triangle optimum configuration, initially enhancing the original idea that symmetrical configurations would yield the optimum configurations. The 3-5 micron contour plot (Figure 18) clearly shows the area that cannot be filled in by using the multiple wavelength MTF information.

All of the comparison tables are arranged as follows: reading across, the percent improvement is between the two configurations being contrasted; reading down, the percent improvement is in the same mirror configuration between the three and three-to-five micron results.

Table 1. Three-Mirror Results

	Symmetrical Configuration	OR Configuration	% Improvement OR vs Symmetrical
3 Micron E.D. (meters)	2.007	2.007	0
3-5 Micron E.D. (meters)	2.007	2.007	0
% Improvement	0	0	

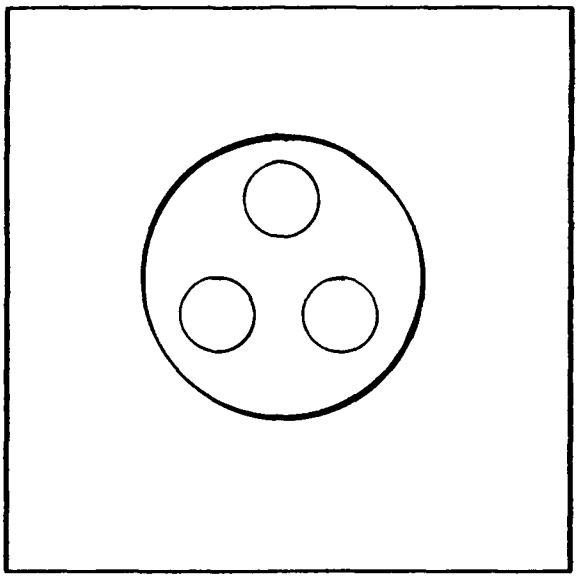

Figure 16. 3-Mirror triangle

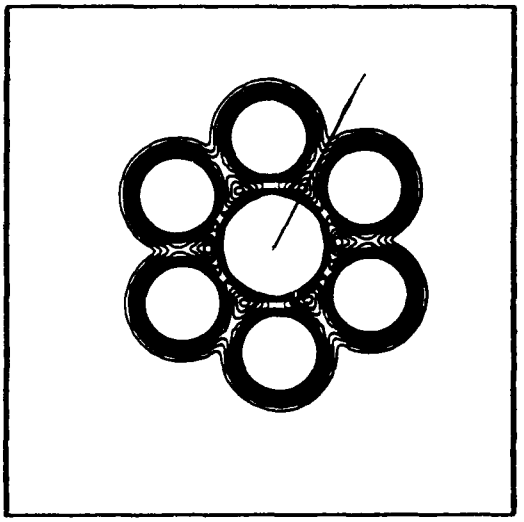

Figure 17. 3-mirror, 3-micron MTF

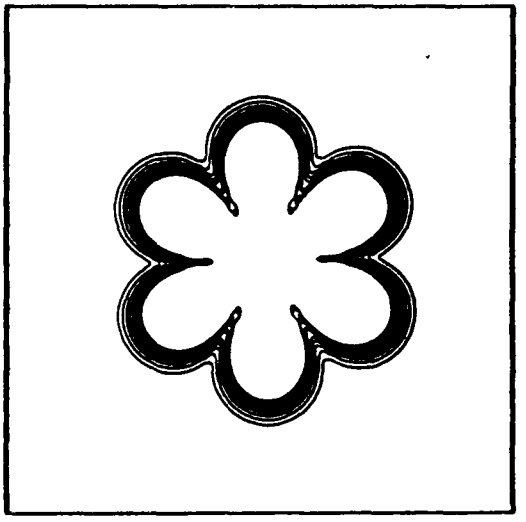

Figure 18. 3-mirror, 3-5 micron MTF

Four-Mirror Cross. For ease of inputting the mirror coordinates, the four-mirror cross was rotated 45 degrees and evaluated as a four-mirror box (Figure 19). The four-mirror configuration yielded a more promising MTF; as seen in Figure 20, the outer MTF rings are not equidistant from the central ring. Because of this arrangement, when going from the 3 micron MTF to the 3-5 micron MTF, the corner MTF rings radially collapse to fill in the points at which the single-wavelength MTF opens up (at the edge of the central MTF ring). This results in an increased equivalent diameter for the three-to-five micron MTF.

As discussed earlier, the OR optimization yielded two significant results. The first was that the optimum configuration the OR routine obtained was better than the symmetrical configuration; the second was that the optimum configuration was not symmetrical.

Table 2. Four-Mirror Results

	Symmetrical Configuration	OR Configuration	% Improvement OR vs Symmetrical
3 Micron E.D. (meters)	2.235	2.644	18.4%
3-5 Micron E.D. (meters)	2.418	2.706	11.9%
% Improvement	8.3%	2.3%	

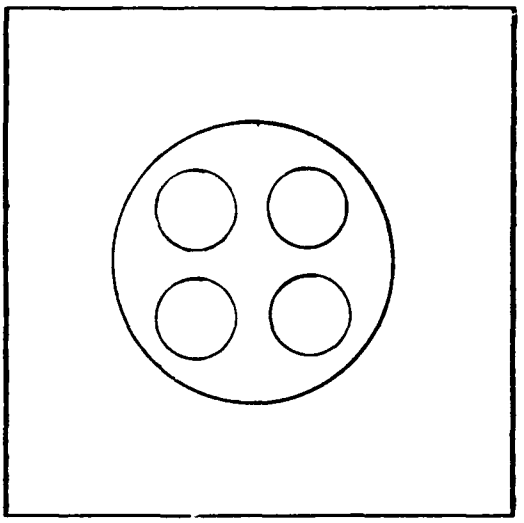

Figure 19. 4-mirror box

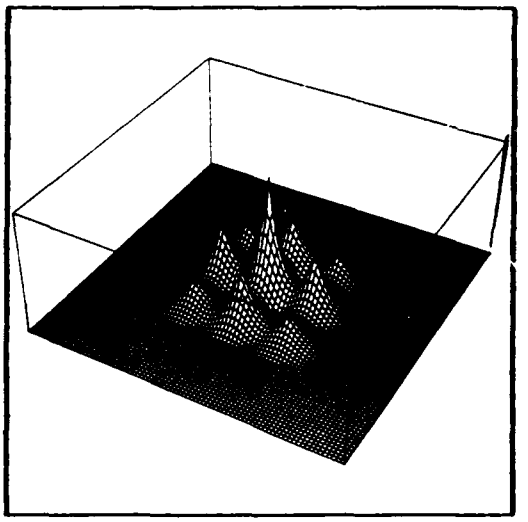

Figure 20. 4-mirror box, 3 micron 3-D plot

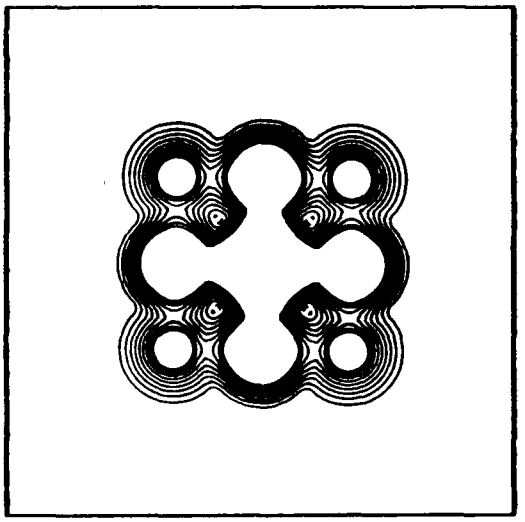

Figure 21. 4-mirror box, 3 micron contour plot

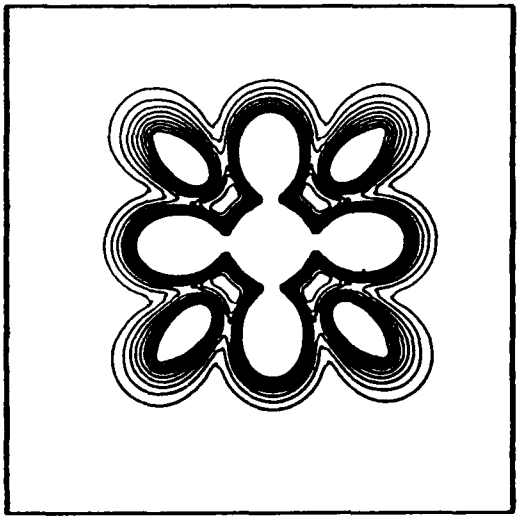

Figure 22. 4-mirror box, 3-5 micron contour plot

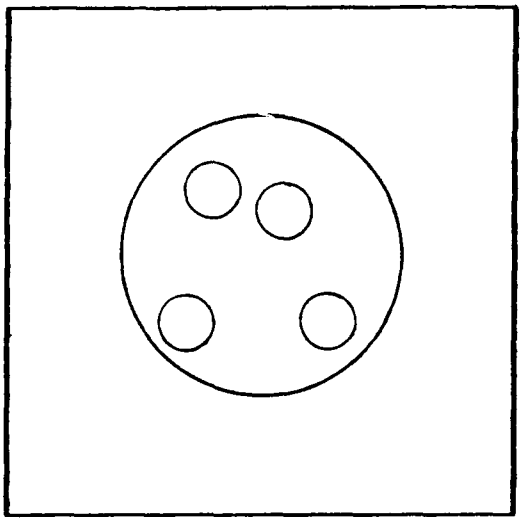

Figure 23. 4-mirror OR optimum, 3-micron

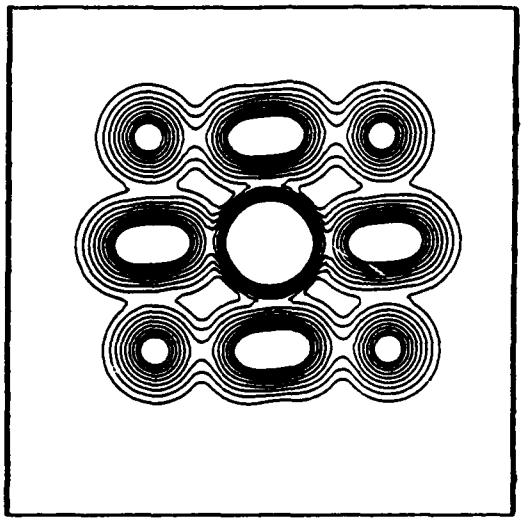

Figure 24. 4 mirror OR optimum, 3 micron contour plot

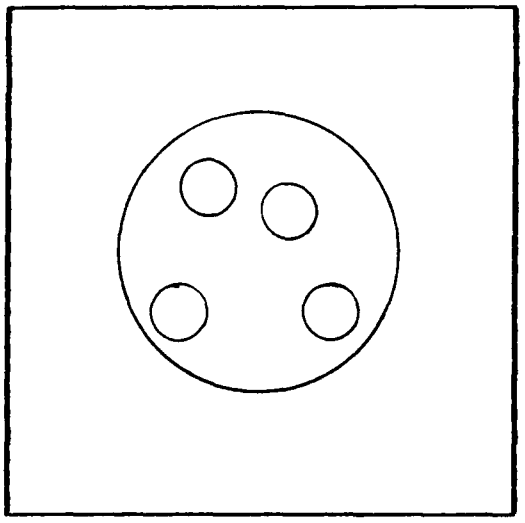

Figure 25. 4-mirror OR optimum , 3-5 micron

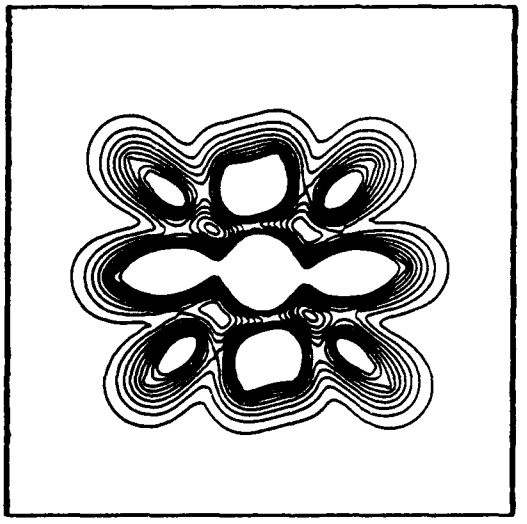

Figure 26. 4-mirror OR optimum, 3-5 micron contour plot

Four-Mirror Cross with Center Mirror. This five-mirror pattern was studied to see if adding a center mirror to the four-mirror cross configuration would improve the four-mirror system's equivalent diameter. There was improvement in the 3-micron MTF value when compared to the four-mirror cross, but only marginal improvement in the three-to five micron MTF as compared to the 4-mirror cross, as shown in Table 3.

There is no benefit in using the five-mirror cross configuration; the 5-mirror pentagon has better results. There was no OR optimization performed on this configuration; the five-mirror system was optimized using a pentagon as a start point.

Table 3. Comparison of 4 vs 5 mirror cross

	Four-mirror Cross	Five-mirror Cross	% Improvement 4 vs 5 Mirror
3 Micron E.D. (meters)	2.235	2.414	8.0%
3-5 Micron E.D. (meters)	2.418	2.431	0.5%
% Improvement	8.3%	0.7%	

Five-Mirror Pentagon. This symmetrical configuration suffers the same problems as the three-mirror equilateral triangle. The middle and outer MTF "rings" are equidistant from the origin; therefore there can be no benefit from using MTF information from the longer wavelengths.

The OR optimization at the single, 3-micron, wavelength did not yield any improvement over the symmetrical values; however, the 3-5 micron run did offer a slightly better value. In plotting the coordinates, it appears that the routine simply improved the placement of the symmetrical pentagon optimum mirror configuration. The results are summarized in Table 4.

The six-mirror pentagon was briefly studied; there was no improvement in the minimum MTF.

Table 4. 5-mirror results

	Symmetrical Configuration	OR Configuration	% Improvement OR vs Symmetrical
3 Micron E.D. (meters)	3.24	3.24	0.0%
3-5 Micron E.D. (meters)	3.24	3.28	1.23%
% Improvement	0.0%	1.23%	

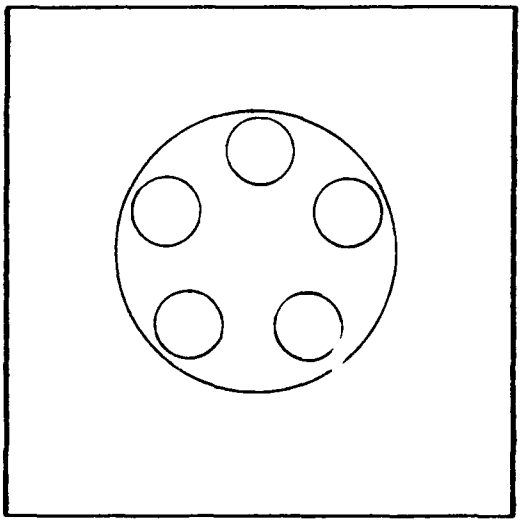

Figure 27. 5-mirror pentagon

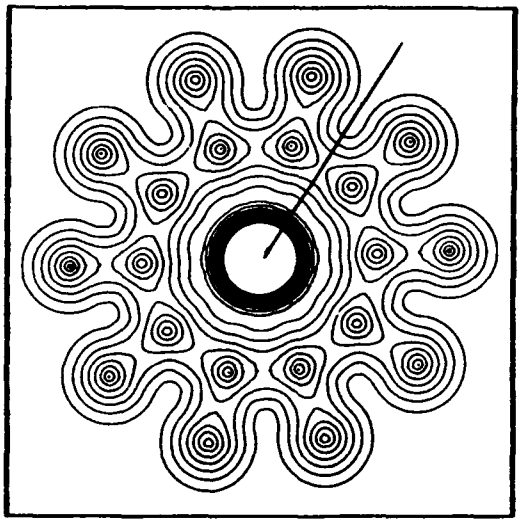

Figure 28. 5-mirror pentagon, 3 micron contour plot

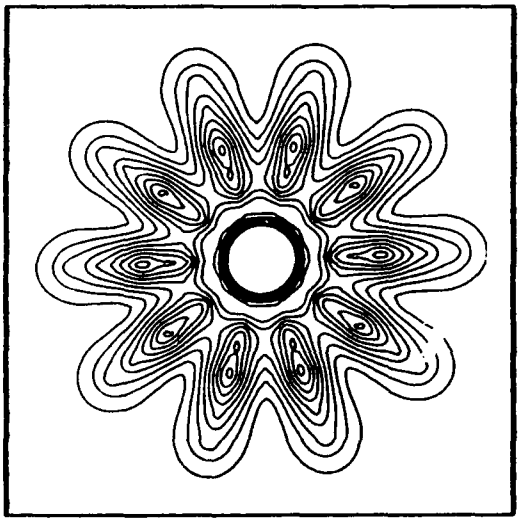

Figure 29. 5-mirror pentagon, 3-5 micron contour plot

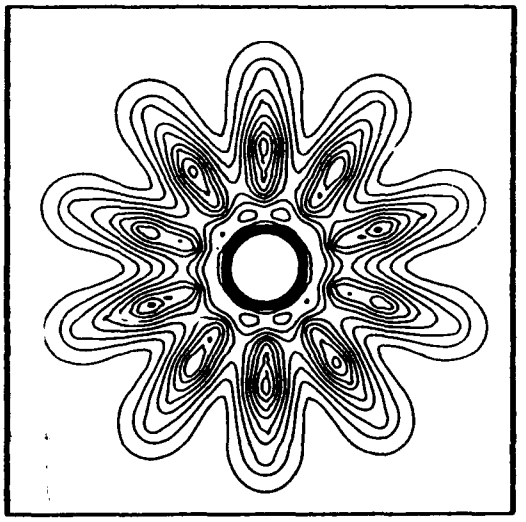

Figure 30. 5-mirror OR optimum, 3-5 micron contour plot

Six-Mirror Configurations. The six-mirror systems proved to be the most complex series of mirror systems to study simply due to the number of mirrors and their resulting many possibilities of arranging the mirror configurations. As with the other mirror numbers, the first goal was to optimize this mirror system using a symmetrical, hexagonal, arrangement. Since the outer rings of this configuration were not equidistant from the origin (Figure 33), the hexagonal configuration could be improved upon by using the multiple wavelength MTF.

Another six-mirror of interest was the six-mirror Golay pattern (Figure 35). As described previously, this unique mirror arrangement results in no ring overlap (Figure 37); since the MTF pattern is highly symmetrical, the minimum MTF value should be fairly high. The Golay configuration did result in a significantly higher minimum MTF for both the single, three micron configuration as well as the three-to-five micron configuration when compared to the symmetrical hexagon values.

The OR optimization of the six-mirror hexagon system resulted in values between the hexagon configuration and the Golay configuration. The Golay pattern was also entered in the optimization routine; this yielded slightly better results than the manual optimization, but the increase in minimum MTF is attributed to the more precise arrangement of the mirrors into the Golay pattern rather than an improvement over the Golay pattern. The values used in the

Golay comparison are the OR optimized results.

The three-dimensional and contour plots of the six-mirror systems are with a maximum spatial frequency of $2 \times 10^6 \ m^{-1}$.

Table 5. Comparison of hexagon and OR optima

	Symmetrical Configuration	OR Configuration	% Improvement OR vs Symmetrical
3 Micron E.D. (meters)	3.579	3.945	10.23%
3-5 Micron E.D. (meters)	3.732	4.114	10.24%
% Improvement	4.27%	4.28%	

Table 6. Comparison of hexagon and Golay optima

	Symmetrical Configuration	Golay Configuration	% Improvement Golay vs Symmetrical
3 Micron E.D. (meters)	3.579	4.344	21.37%
3-5 Micron E.D. (meters)	3.732	4.694	25.77%
% Improvement	4.27%	8.06%	

Table 7. Comparison of OR and Golay optima

	OR Configuration	Golay Configuration	% Improvement Golay vs OR
3 Micron E.D. (meters)	3.945	4.344	10.11%
3-5 Micron E.D. (meters)	4.114	4.694	14.10%
% Improvement	4.28%	8.06%	

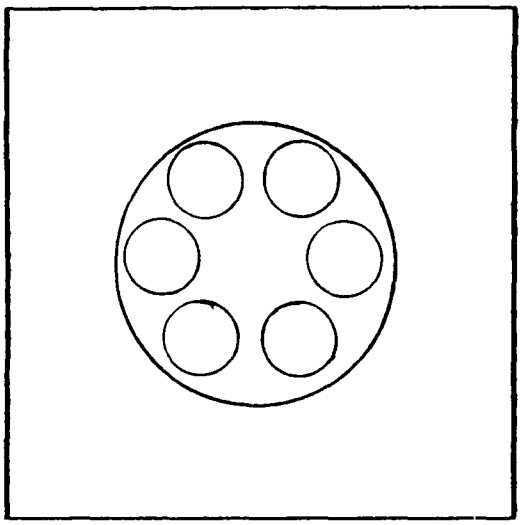

Figure 31. 6-mirror hexagon

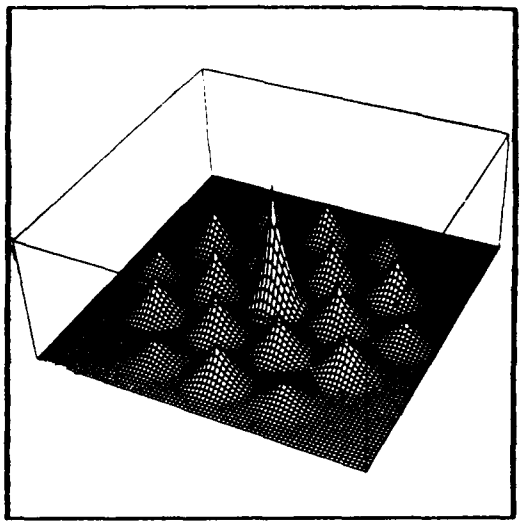

Figure 32. 6-mirror hexagon, 3 micron 3-D plot

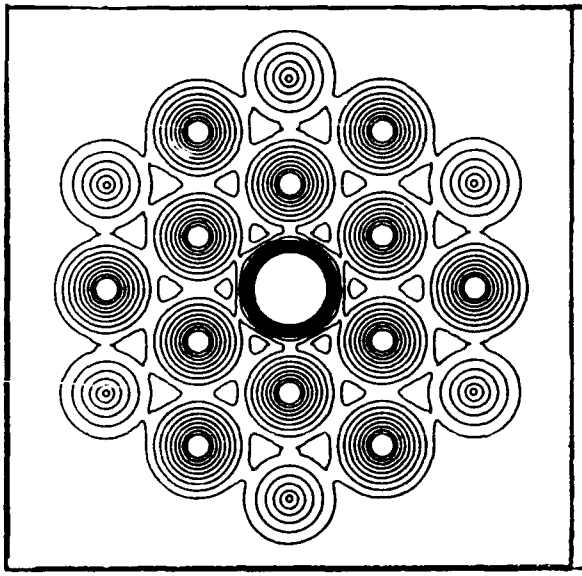

Figure 33. 6-mirror hexagon, 3 micron contour plot

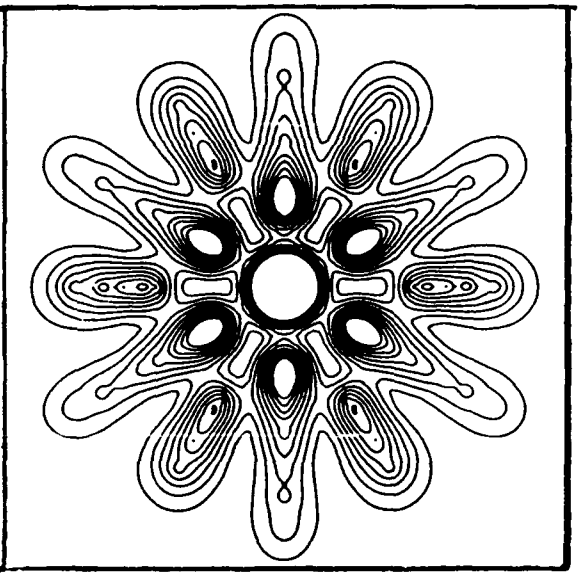

Figure 34. 6-mirror hexagon, 3-5 micron contour plot

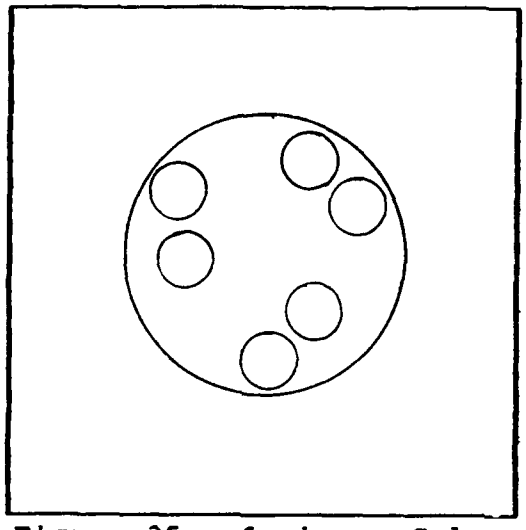

Figure 35. 6-mirror Golay

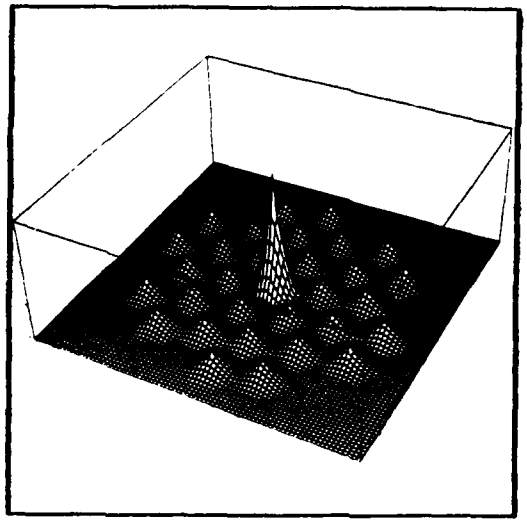

Figure 36. 6-mirror Golay, 3 micron 3-D plot

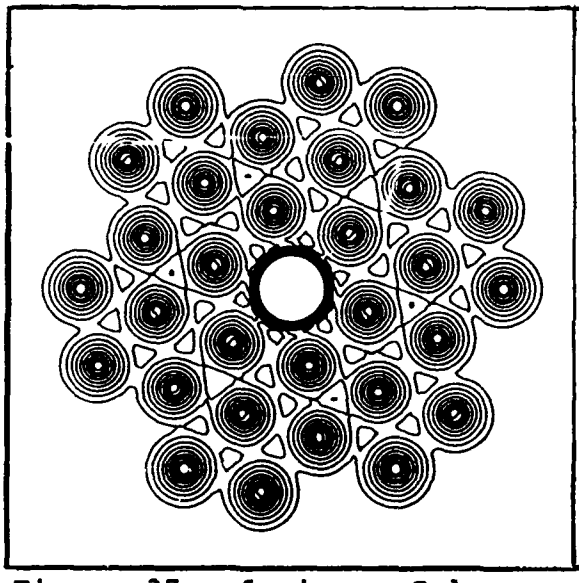

Figure 37. 6-mirror Golay, 3 micron contour plot

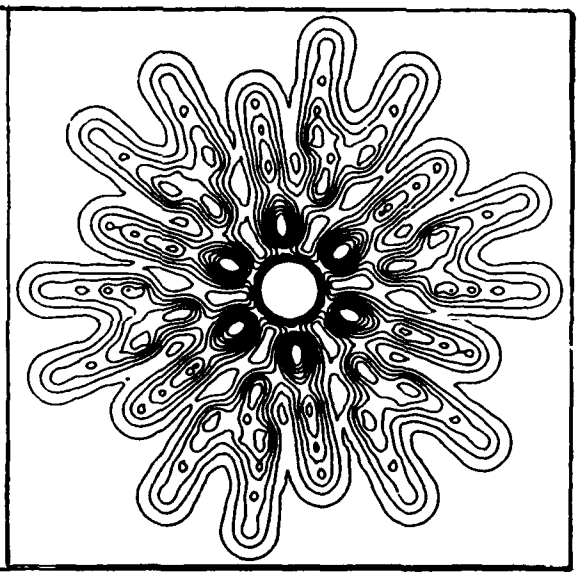

Figure 38. 6-mirror Golay, 3-5 micron contour plot

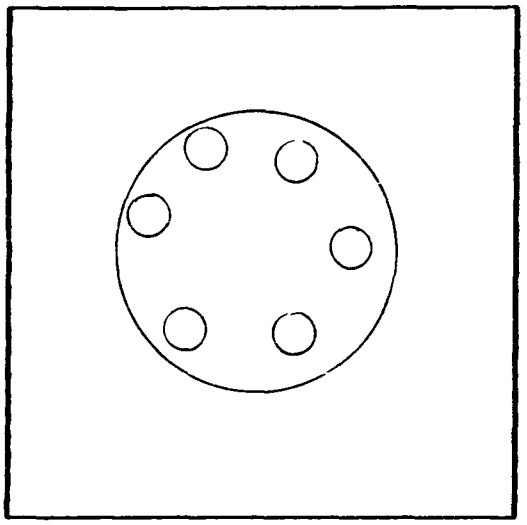

Figure 39. 6- mirror OR optimum, 3 micron

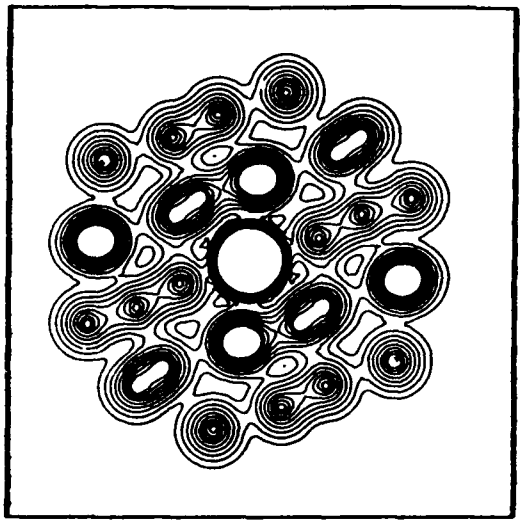

Figure 40. 6-mirror OR optimum, 3 micron contour plot

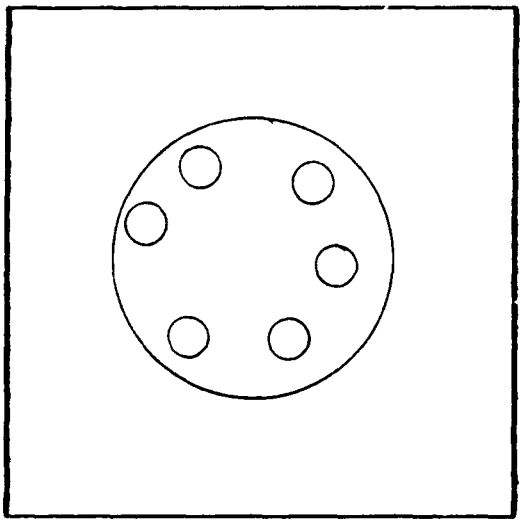

Figure 41. 6-mirror OR optimum, 3-5 micron

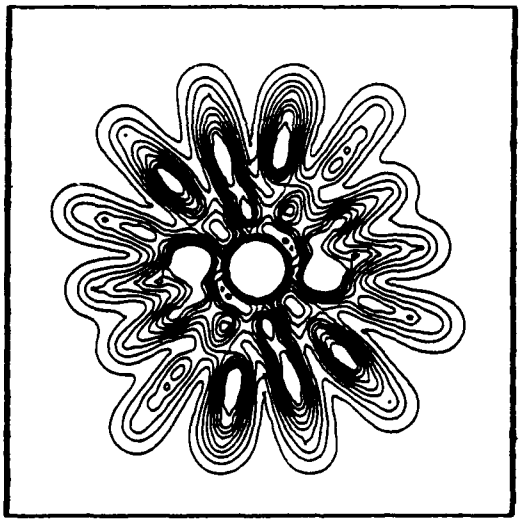

Figure 42. 6-mirror OR optimum, 3-5 micron contour plot

Qualitative Comparison of Golay 6 Resolution

This analysis of the Golay six mirror configuration was made using the OR optimized Golay mirror configuration. The analysis was performed in three runs: the first run used the single, three micron optimum configuration, the second run used the single wavelength mirror coordinates but used the three-to-five micron wavelength spread, and the third run used the three-to-five micron OR optimum configuration. All the runs used a simulated one-meter disk at 500,000 meters as the target. The Fortran code used in this series of runs is included in Appendix E.

The results showed an increase in resolution from the single, three micron configuration compared to the three-to-five micron configuration. Figure 43 graphs a crosscut of two images; the low peak line is the single wavelength cylinder cross-section, the high peak is the multiple wavelength cylinder cross-section. The single and multiple wavelength MTF plots are compared in Figure 44.

The results from this series of runs is a good first indication that the resolution does increase when using the multiple wavelength technique; however, the results are strictly qualitative.

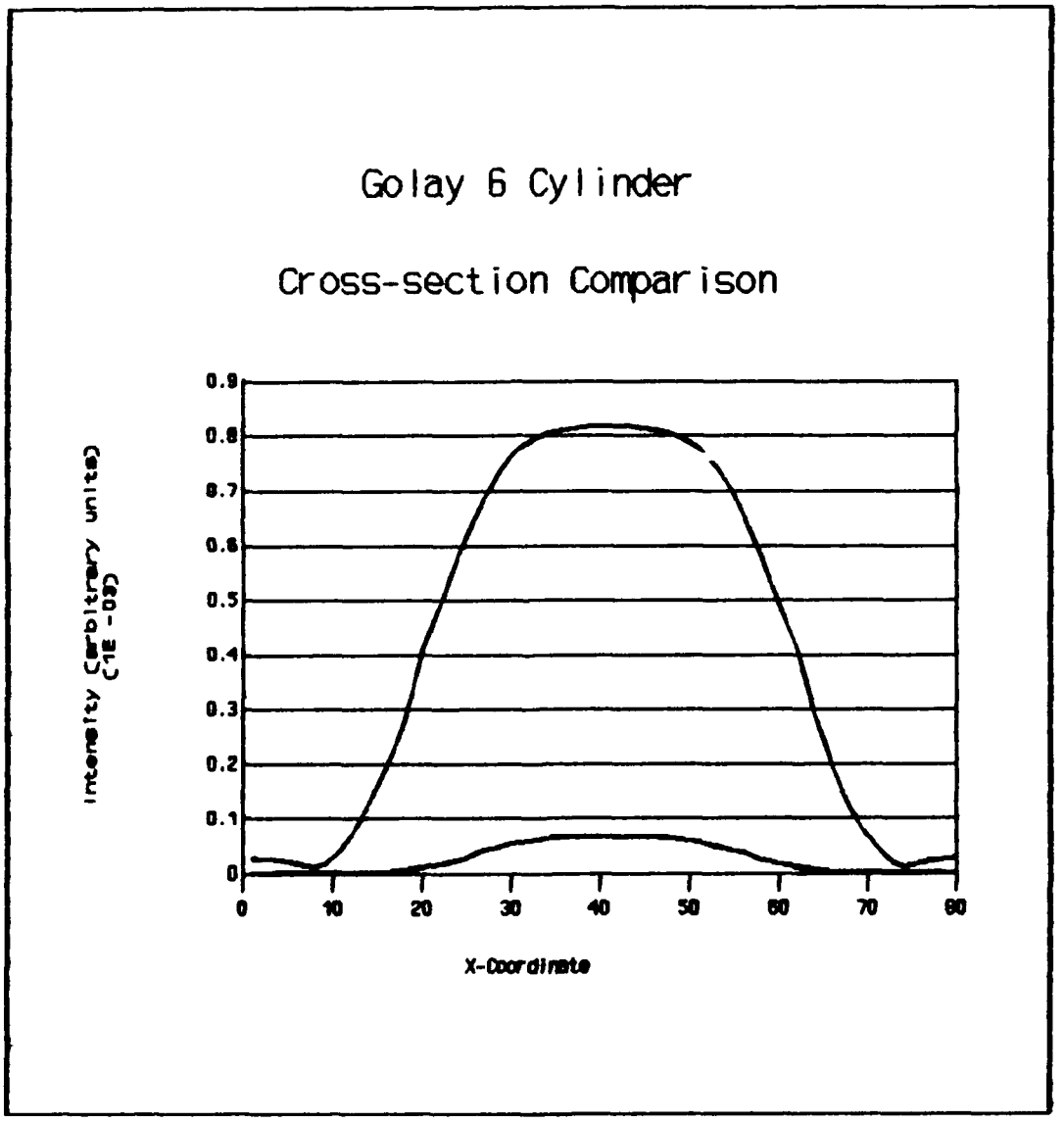

Figure 43. Comparison of two Golay 6 cylinder cross-sections

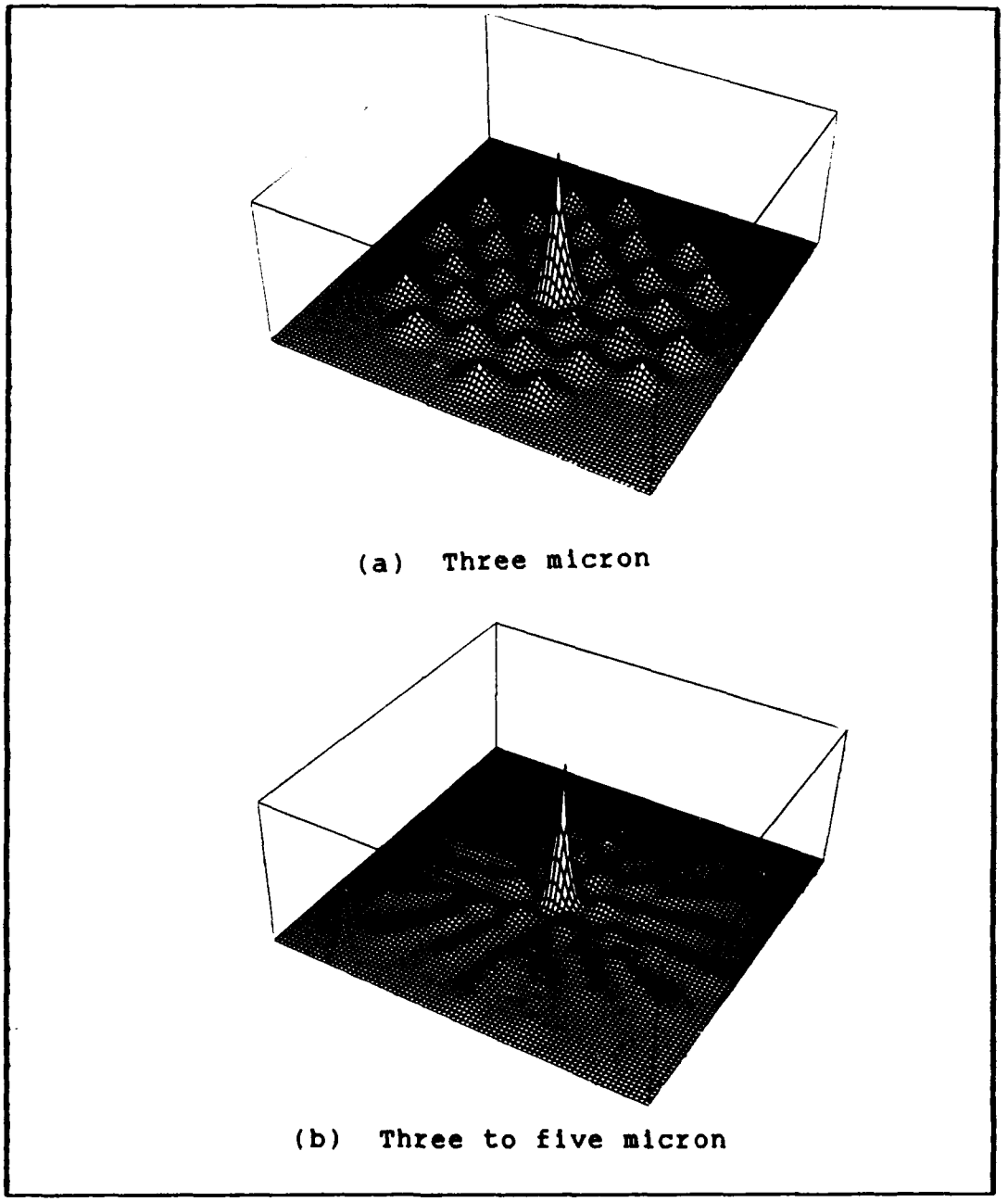

(a) Three micron

(b) Three to five micron

Figure 44. Comparison of Golay 6 3 and 3-5 micron MTF

V. Conclusions

Summary

The goal of this thesis was to study the possibility of increasing the theoretical spatial resolution of various multiple mirror systems by using spatial information gathered over a broad wavelength spectrum. This task was accomplished in several stages. First, the criterion for determining a system's maximum spatial resolution was established by using Harvey's criterion of the maximizing the spatial frequency at which the system observed its first zero in the MTF, referred to as "minimum MTF" throughout the thesis. The second stage was to choose several multiple mirror configurations for study. The thesis studied three through six mirror systems, choosing a symmetrical configuration within each particular number of mirrors in the belief that symmetry would yield the best results. Each chosen system was manually optimized at three microns by slowly increasing the distance between mirrors until an interior zero opened up in the system. At that point, the three-to-five micron spectrum was optimized, again by slowly increasing the distance between mirrors until an interior zero opened up in the interior of the MTF. Afterwards, each mirror system was optimized using an Operations Research optimization routine and compared to the symmetrical mirror systems with the same number of mirrors. Finally, an initial attempt was made in determining the significance of

the increased minimum MTF between single wavelength and multiple wavelength results of a particular mirror system.

General Conclusions

The main goal was to use spectral information from a wavelength spectrum to increase a system's resolving capability over the system's capability at a single wavelength. A significant increase was realized in all symmetrical, even-numbered mirror configurations. The odd number mirror configurations did not show an increase in resolution because their resulting MTF patterns were aligned equidistant from the center ring and, as the wavelength increased, the system collapsed radially inward. At the same time, the MTF rings became smaller, not allowing the gathered information to fill in the interior zeros that developed when the mirrors were moved apart.

The Operations Research optimization routine was quite successful in discovering nonsymmetrical configurations that increased the system's resolving capability over its symmetrical counterpart.

The significance in the increased spatial resolution is strictly qualitative. The initial results show that there is an increase in the resolving capability of a system using the multiple wavelength technique, as originally hypothesized.

Recommendations

This thesis lays the foundation for using a wavelength spectrum in conjunction with multiple mirrors to increase a system's overall resolution. Theoretically, this thesis demonstrated the validity of this assumption. There are several practical aspects that still need consideration.

The first aspect is the criterion used for evaluating the mirror systems. Harvey's criterion was a good starting point, but there could be a better criterion developed that more appropriately represents the higher spatial frequency information gathered.

A second aspect is the practical determination of the increase in spatial resolution between the single and multiple wavelength results of a particular system. The initial results indicated an increase in resolution. Further studies could concentrate on a more quantitative approach to validating this result.

A third area of future research is refining the Operations Research optimization routine to improve its probability of finding global optima for the various mirror configurations studied.

APPENDIX A: MAIN PROGRAM USED IN GENERATING MTF

```
C
C   This main program generates an MTF array and evaluates
C   the matrix to determine the minimum MTF in the
C   array.  Data is read from file "init.val" and
C   the results are entered in file "answer".
C
      REAL X(10),Y(10),LAMDA1,R,XI,ETA,STEP,LSTEP,P
      REAL RVAL,MTFMIN,XIP,ETAP,RUNNUM,MAXVAL
      REAL MTF(-150:150,-150:150),PI,DELX,DELY,LAMDA2
      INTEGER I,J,K,L,M,N,A,B
      OPEN (11,FILE='init.val',STATUS='OLD')
      OPEN (12,FILE='answer',STATUS='OLD')
      PI=3.141592654
C
C  This portion reads in data from file "init.val" created
C  by the program "values"
C
C  INPUTS:
C
C          N = (integer)  Number of mirrors.
C X(I), Y(I) = (meters) Cartesian coordinates of the
C                  mirrors
C    LAMDA1   = (microns) Shortest wavelength.
C    LAMDA2   = (microns) Longest wavelength.
C    LSTEP    = In multiple wavelength runs, the step
C               increase in wavelength.
C    RUNNUM   = Run number.
C    MAXVAL   = (microns) Maximum desired spatial value.
C
      READ(11,*) N
      DO 10 I = 1,N
         READ(11,*) X(I),Y(I)
   10  CONTINUE
      READ(11,*) LAMDA1,LAMDA2
      READ(11,*) LSTEP
      READ (11,*) RUNNUM
      READ (11,*) MAXVAL
      STEP = MAXVAL / 150.0
      DO 60 P = LAMDA1,LAMDA2,LSTEP
         DO 50 J = 1,N
            DO 40 K = 1,N
               DELX = X(J)-X(K)
               DELY = Y(J)-Y(K)
               XI = -MAXVAL
               ETA = -MAXVAL
               DO 30 L = -150,150
                  DO 20 M = -150,150
                     R = SQRT(((P * XI) - DELX) **2
     *                    + ((P * ETA) - DELY) **2)
                     IF (R.GT.1) THEN
                        MTF(M,L)=MTF(M,L)
```

```
                              ELSE
                              MTF(M,L) = 2 / PI * (ACOS(R)
     *                        -SQRT(R * (1-R **2))) + MTF(M,L)
                            END IF
                            XI = XI + STEP
    20                    CONTINUE
                          ETA = ETA + STEP
                          XI = -MAXVAL
    30                  CONTINUE
    40                CONTINUE
    50            CONTINUE
    60    CONTINUE
          WRITE (12,*) 'MTF AT 0,0 IS ',MTF(0,0)
C
C   This portion calculates the minimum zero value of a
C                       given MTF profile
C
          MTFMIN = 5.0
          DO 100 B = -150,150
             DO 90 A = -150,150
                IF (MTF(A,B).GT.0) THEN
                   GO TO 90
                   ELSE
                   XI = STEP * A
                   ETA = STEP * B
                   RVAL = SQRT(XI**2 + ETA**2)
                   IF (RVAL.LT.MTFMIN) THEN
                      MTFMIN = RVAL
                   XIP = XI
                   ETAP = ETA
                   END IF
                END IF
    90       CONTINUE
   100    CONTINUE
C
C   This portion writes the result into file "answer"
C
C
          WRITE (12,*) 'MIN MTF IS',MTFMIN
          WRITE (12,*) XIP
          WRITE (12,*) ETAP
          WRITE (12,*) 'THIS IS RUN NUMBER',RUNNUM
          CLOSE (11)
          CLOSE (12)
          END
```

APPENDIX B: CODE TO WRITE INPUT FOR MAIN PROGRAM

```
C
C
C  This program writes initial values for MTF calculations
C   into file "init.val" for use in main program
C
C  INPUTS:
C
C  N               = (integer) Number of mirrors in the pupil
C  X(I),Y(I)       = (real,meters) coordinate of mirror in
C                    Cartesian Coordinate system
C  LAMDA1, LAMDA2  = (real,microns) wavelength range of MTF
C  LSTEP           = (real,microns) step interval in multiple
C                    wavelength MTF calculation
C  MAXVAL          = (real,microns) maximum array value
C
C
C
      REAL X(10),Y(10),LAMDA1,LAMDA2,LSTEP,RUNNUM,MAXVAL
      INTEGER I,N
      OPEN(10,FILE='init.val',STATUS='OLD')
      PRINT *,'ENTER NUMBER OF APERTURES'
      READ *,N
      WRITE (10,*) N
      DO 10 I = 1,N
         PRINT *,'ENTER COORDINATES OF APERTURE ',I
         READ *,X(I), Y(I)
         WRITE (10,*) X(I), Y(I)
10    CONTINUE
      PRINT *,'ENTER WAVELENGTH MIN AND MAX VALUES (IN
     *MICRONS)'
      READ *,LAMDA1,LAMDA2
      WRITE (10,*) LAMDA1,LAMDA2
      PRINT *,'ENTER WAVELENGTH STEP SIZE (IN MICRONS)'
      READ *,LSTEP
      WRITE (10,*) LSTEP
      PRINT *,'ENTER RUN NUMBER'
      READ *,RUNNUM
      WRITE (10,*) RUNNUM
      PRINT *,'ENTER MAX SPATIAL VALUE (FOR ZOOM RUN)'
      READ *, MAXVAL
      WRITE (10,*) MAXVAL
      CLOSE (10)
      END
```

APPENDIX C: OPTIMIZATION CODE

```
      REAL X(10),Y(10),LAMDA1,LAMDA2,STEP,LSTEP
      REAL TSTEP,TDONE,RSTEP,R(10),RH(10),THETAH(10)
      REAL ANSPR,ANSNR,ANSPT,ANSNT,ANS,RDONE,THETA(10)
      REAL RUNNUM,MAXVAL,PI
      INTEGER I,N,COUNT

      DATA PI/3.141592654/

      OPEN (11,FILE='input.or',STATUS='OLD')
      OPEN (12,FILE='optim',STATUS='OLD')
      READ(11,*) N

      DO 10 I = 1,N
         READ(11,*) R(I),THETA(I)
   10  CONTINUE

      READ(11,*) LAMDA1,LAMDA2
      READ(11,*) LSTEP
      READ (11,*) RUNNUM
      READ (11,*) MAXVAL
      READ (11,*) RDONE
      READ (11,*) TDONE
      STEP = MAXVAL / 150.0
      TSTEP = .1
      RSTEP = .1
      CALL PLR2XY(N,THETA,R,X,Y)
      WRITE (12,*) 'THIS IS RUN NUMBER',RUNNUM
      WRITE (12,*) 'INITIAL X AND Y VALUES ARE'
      DO 3 I = 1,N
         WRITE (12,*) X(I),Y(I)
    3  CONTINUE
      ANS = RMTRMN(N,X,Y,LAMDA1,LAMDA2,LSTEP,MAXVAL,STEP)
      WRITE (12,*) 'INITIAL MTF IS',ANS
  100 IF((TSTEP.LE.TDONE).AND.(RSTEP.LE.RDONE)) GO TO 200

      DO 15 I = 2,N
   20    RH(I) = R(I)
         THETAH(I) = THETA(I)
C
C        Radius steps outward
C
         R(I) = RH(I) + RSTEP
         CALL PLR2XY(N,THETA,R,X,Y)
         ANSPR=RMTFMN(N,X,Y,LAMDA1,LAMDA2,LSTEP,MAXVAL,STEP)

C
C         The next step determines if the resulting minimum
C         MTFis better than the previous best MTF
C
C
         IF (ANSPR.GE.ANS) THEN
            ANS = ANSPR
```

```
            ELSE
C
C       If outward does not improve minval, radius steps in
C
            R(I) = RH(I)-RSTEP
            CALL PLR2XY(N,THETA,R,X,Y)
            ANSNR = RMTFMN(N,X,Y,LAMDA1,LAMDA2,
     *              LSTEP,MAXVAL,STEP)
C
C      Check for increase in Minval
C
            IF (ANSNR.GT.ANS) THEN
               ANS = ANSNR
               ELSE
               R(I) = RH(I)
            END IF
          END IF
C
C       With the radial direction checked, the theta
C       direction is checked in both negative and
C       positive direction.
C          Theta(2) is always zero, thus the following IF
C       statement.
C
          IF (I.EQ.2) GO TO 15
          THETA(I) = THETAH(I)-TSTEP
          CALL PLR2XY(N,THETA,R,X,Y)
          ANSNT = RMTFMN(N,X,Y,LAMDA1,LAMDA2,
     *            LSTEP,MAXVAL,STEP)
          IF (ANSNT.GE.ANS) THEN
             ANS = ANSNT
             ELSE
             THETA(I) = THETAH(I)+TSTEP
             CALL PLR2XY(N,THETA,R,X,Y)
             ANSPT = RMTFMN(N,X,Y,LAMDA1,LAMDA2,
     *               LSTEP,MAXVAL,STEP)
             IF (ANSPT.GT.ANS) THEN
                ANS = ANSPT
                ELSE
                THETA(I) = THETAH(I)
             END IF
          END IF
C
C    Did the mirror move?  If no, on to the next mirror.
C    Else we try to move the same mirror again.
C
C
   15  CONTINUE
C
C  The next portion check to see if ANY of the mirrors moved
C  in the latest iteration.  If none moved, the step size is
C  halved. If yes, go through the entire iteration again
C  with the same step.
C
       COUNT = 0
```

```
      DO 40 I = 2,N
       IF ((R(I).EQ.RH(I)).AND.(THETA(I).EQ.THETAH(I))) THEN
          COUNT = COUNT + 1
       END IF
 40    CONTINUE
       IF (COUNT.EQ.(N-1)) THEN
          TSTEP = TSTEP / 2
          RSTEP = RSTEP / 2
          GO TO 100
       ELSE
          GO TO 100
       END IF

 200   WRITE (12,*) 'MINVAL IS', ANS
       WRITE (12,*) 'AT MIRROR LOCATION'
       CALL PLR2XY(N,THETA,R,X,Y)
       DO 50 I = 1,N
          WRITE (12,*) X(I),Y(I)
 50    CONTINUE
       WRITE (12,*) 'THIS IS RUN NUMBER',RUNNUM
       CLOSE (11)
       CLOSE (12)
       END

       SUBROUTINE PLR2XY(N,THETA,R,X,Y)
C
C  This subroutine converts from a polar description of the
C  mirror configuration to an (X,Y) description.
C
C  INPUTS:
C     N          = (integer) Number of mirrors (must be >=3).
C     THETA(I)   = (real,radians) Angle from mirror(i-1) to
C                  mirror(i).
C                  THETA(1) is never used.
C                  THETA(2) is always 0.0.
C     R(I)       = (real,meters) Distance from mirror(i-1) to
C                  mirror(i).
C                  R(1) is never used.
C  OUTPUTS:
C     X(i)       = (real,meters) X coordinate of mirror(i).
C     Y(i)       = (real,meters) Y coordinate of mirror(i).
C
C  LOGIC:
C     Compute each mirror in turn, using trigonometry.
C        X(i)=X(i-1) + R(i)*COS(THETA(i))
C        Y(i)=Y(i-1) + R(i)*SIN(THETA(i))
C

       DIMENSION THETA(10),R(10),X(10),Y(10)

       X(1) = 0.0
       Y(1) = 0.0

       X(2) = R(2)
       Y(2) = 0.0
```

```
      DO 10 I = 3,N
         IOLD = I-1
         X(I) = X(IOLD)+R(I)*COS(THETA(I))
         Y(I) = Y(IOLD)+R(I)*SIN(THETA(I))
10     CONTINUE

      RETURN
      END

      Real Function RMTFMN(N,X,Y,LAMDA1,LAMDA2,
     *                     LSTEP,MAXVAL,STEP)
      INTEGER I,J,K,L,M,N,A,B
      Real LAMDA1,LAMDA2,PI
      REAL R,XI,ETA,STEP,LSTEP,P
      REAL RVAL,RMTFMN,XIP,ETAP,MAXVAL
      REAL MTF(-150:150,-150:150),PI,DELX,DELY,LAMDA2

      Dimension X(10),Y(10)

      DATA PI/3.141592654/

      DO 10 I = -150,150
        DO 10 J = -150,150
           MTF(I,J) = 0.0
10       CONTINUE

      DO 60 P = LAMDA1,LAMDA2,LSTEP
        DO 50 J = 1,N
           DO 40 K = 1,N
              DELX = X(J)-X(K)
              DELY = Y(J)-Y(K)
              XI = -MAXVAL
              ETA = -MAXVAL
              DO 30 L = -150,150
                 DO 20 M = -150,150
                  R = SQRT(((P * XI) - DELX)**2
     *                    + ((P*ETA) - DELY)**2)
                   IF(R.GT.1) THEN
                     MTF(M,L) = MTF(M,L)
                     ELSE
C
C    Normally the following equation is used to compute
C    the value of the MTF at the given R value.  To save
C    computer time, if there is a value to be placed in the
C    MTF position, we place a 1.
C
C                      MTF(M,L) = 2 / PI * (ACOS(R)
C    *                           - SQRT(R * (1 - R**2)))
C    *                           + MTF(M,L)
C
                       MTF(M,L) = 1 + MTF(M,L)
                     END IF
                     XI = XI + STEP
20                   CONTINUE
                  ETA = ETA + STEP
```

```
                XI = -MAXVAL
   30           CONTINUE
   40         CONTINUE
   50       CONTINUE
   60    CONTINUE

C
C  This portion calculates the minimum zero values of a
 C                   given MTF profile
 C

      RMTFMN = 5.0
      DO 100 B = -150,150
      DO 90 A = -150,150
            IF (MTF(A,B).GT.0) THEN
               GO TO 90
               ELSE
               XI = STEP * A
               ETA = STEP * B
               RVAL = SQRT(XI**2 + ETA**2)
                IF (RVAL.LT.RMTFMN) THEN
                     RMTFMN = RVAL
                     XIP = XI
                     ETAP = ETA
                END IF
            END IF
   90    CONTINUE
  100 CONTINUE
      RETURN
      END
```

APPENDIX D: COORDINATES OF MIRROR SYSTEMS

This appendix details the Cartesian coordinates of the optimum mirror configurations as described in Chapter 4. Since the only concern was relative mirror position, the various input coordinates were varied for ease of input, rather than being concerned with standard input parameters, for example, symmetry about the origin. The coordinates presented in this appendix are the center points of one-meter diameter mirrors with all the coordinates having units of meters.

Three-Mirror Configuration

The three-mirror configuration yielded only one configuration -- the equilateral triangle. As stated in Chapter 4, there was no improvement in the MTF between the three-micron and three-to-five micron runs.

Table 8.

3-Mirror equilateral triangle

x	y
1.0	0.0
-0.5	0.866
-0.5	-0.866

Four-Mirror Configurations

Table 9.

Symmetrical optimum 4-mirror cross, 3 micron

x	y
0.7	0.7
0.7	-0.7
-0.7	0.7
-0.7	-0.7

Table 10.

OR optimum 4-mirror, 3 micron

x	y
0.0	0.0
2.263	0.0
1.871	1.680
0.508	1.724

Table 11.

Symmetrical optimum 4-mirror cross, 3-5 micron

x	y
0.91	0.91
0.91	-0.91
-0.91	0.91
-0.91	-0.91

Table 12.

OR optimum 4-mirror, 3-5 micron

x	y
0.0	0.0
2.344	0.0
1.884	1.718
0.324	1.887

Five-Mirror Configurations

Table 13.

Symmetrical 4-mirror cross with center mirror, 3 micron

x	y
0.0	0.0
0.9	0.9
0.9	-0.9
-0.9	0.9
-0.9	-0.9

Table 14.

Symmetrical 4-mirror cross with center mirror, 3-5 micron

x	y
0.0	0.0
0.925	0.925
-0.925	0.925
0.925	-0.925
-0.925	-0.925

As discussed in Chapter 4, the pentagon's MTF did not improve between the three micron and the three-to-five micron runs in the symmetrical configuration.

Table 15.

5 mirror pentagon

x	y
1.62	0.0
0.501	1.541
-1.311	0.952
-1.311	-0.952
0.501	-1.541

The OR optimization did give a slightly better minimum MTF value; the coordinates of this configuration follow.

Table 16.

5-mirror OR optimum, 3-5 micron

x	y
0.0	0.0
1.813	0.0
2.343	1.733
0.915	2.850
-0.541	1.770

Six-Mirror Configurations

Table 17.

6-mirror hexagon, 3 micron

x	y
1.70	0.0
0.85	1.472
-0.85	1.472
-1.70	0.0
-0.85	-1.472
0.85	-1.472

Table 18.

6-mirror OR optimum, 3 micron

x	y
0.0	0.0
1.713	0.0
2.653	1.622
2.160	3.092
0.396	3.455
-0.982	2.414

Table 19.

6-mirror Golay, 3 micron

x	y
2.60	0.0
-1.30	2.252
-1.30	-2.252
1.434	1.247
-1.800	0.619
0.363	-1.865

Table 20.

6-mirror hexagon, 3-5 micron

x	y
1.970	0.0
0.985	1.706
0.985	1.706
1.97	0.0
0.985	-1.706
0.985	-1.706

Table 21.

6-mirror OR optimum, 3-5 micron

x	y
0.0	0.0
1.928	0.0
2.900	1.682
2.604	3.370
0.795	3.783
-0.953	2.891

Table 22.

6-mirror Golay, 3-5 micron

x	y
3.0	0.0
-1.5	2.599
-1.5	-2.599
1.811	1.575
-2.270	0.781
0.458	-2.356

Table 23.

OR optimized Golay 6, 3 micron

x	y
0.0	0.0
1.753	0.0
4.255	1.547
3.355	3.037
0.772	4.451
-0.111	2.974

Table 24.

OR optimized Golay 6, 3-5 micron

x	y
0.0	0.0
1.782	0.0
3.880	1.956
3.279	3.562
0.478	4.513
-0.767	3.167

```
C
C    This program generates a 3-dimensional resultant image
C    (file name "data"), and a 1-dimensional slice of that
C    image for examination (file name "line").  This
C    program requires access to the IMSL library (version
C    9.2) to generate the sombrero function and perform the
C    inverse Fourier Transform.
C
      DOUBLE PRECISION X(10),Y(10),LAMDA1,R,XI,ETA
      DOUBLE PRECISION RUNNUM,MAXVAL,STEP,LSTEP,P,DIST
      DOUBLE PRECISION MTF(-40:40,-40:40),PI,DELX,DELY
      DOUBLE PRECISION PVAL,CIRCLE(-40:40,-40:40)
      DOUBLE PRECISION MMBSJ1,ARG,RWK(536),Z,LAMDA2
      INTEGER IA1,IA2,N1,N2,N3,IJOB,IWK(536)
      INTEGER I,J,K,L,M,N,IER
      DOUBLE COMPLEX A(80,80),CWK(81),F(80,80)
      COMPLEX D(80,80)
      OPEN (10,FILE='data',STATUS='NEW')
      OPEN (11,FILE='init.val',STATUS='OLD')
      OPEN (12,FILE='line',STATUS='NEW')
      DATA PI/3.141592654/
      READ(11,*) N
      DO 10 I = 1,N
         READ(11,*) X(I),Y(I)
10    CONTINUE
C
C  Inputs:
C    All inputs are as in previous programs, except
C
C      Dist = (real,meters) distance of 1-meter circle from
C             mirror configuration
C
      READ(11,*) LAMDA1,LAMDA2
      READ(11,*) LSTEP
      READ (11,*) RUNNUM
      READ (11,*) MAXVAL
      READ (11,*) DIST
      DIST = 1/DIST
      STEP = MAXVAL / 40.0
C
C  Generate the appropriate MTF
C
      DO 60 P = LAMDA1,LAMDA2,LSTEP
         DO 50 J = 1,N
            DO 40 K = 1,N
               DELX = X(J) - X(K)
               DELY = Y(J) - Y(K)
               XI = -MAXVAL
               ETA = -MAXVAL
               DO 30 L = -40,40
                  DO 20 M = -40,40
                     R = SQRT(((P * XI) - DELX)**2
```

```
     *                    + ((P * ETA) - DELY)**2)
                       IF (R.GT.1) THEN
                          MTF(M,L) = MTF(M,L)
                          ELSE
                          MTF(M,L) = 2 / PI * (ACOS(R)
     *                                -SQRT(R*(1-R**2)))+MTF(M,L)
                       END IF
                       XI = XI + STEP
  20                CONTINUE
                    ETA = ETA + STEP
                    XI = -MAXVAL
  30              CONTINUE
  40            CONTINUE
  50          CONTINUE
  60        CONTINUE
            MAXVAL = MAXVAL * 1E6
            STEP = MAXVAL / 40
            XI = -MAXVAL
            ETA = -MAXVAL
C
C     Generate appropriate sombrero function
C
            DO 31 L = -40,40
               DO 21 M = -40,40
                  R = SQRT((P * XI)**2 + (P * ETA)**2)
                IF (R.EQ.0) THEN
                   CIRCLE (M,L) = CIRCLE(M-1,L-1)
                   GO TO 21
                END IF
                  ARG = PI*R * DIST
                Z = MMBSJ1(ARG,IER)
                CIRCLE(M,L) = ((2*Z)/(PI*R*DIST))*(PI/4)
                  XI = XI + STEP
  21           CONTINUE
               ETA = ETA + STEP
               XI = -MAXVAL
  31        CONTINUE
C
C     Find the maximum MTF value for normalization
C
            DO 110 J = -40,40
               DO 110 I = -40,40
                  IF (MTF(I,J).GT.PVAL) PVAL = MTF(I,J)
 110        CONTINUE
C
C     Normalizing matrix
C
            DO 200 J = -40,40
               DO 200 I = -40,40
                  MTF(I,J) = MTF(I,J) / PVAL
 200        CONTINUE

C     Multiplying matrices together
C
            DO 300 J = -40,39
```

```
            L = J + 41
            DO 300 I = -40,39
               K = I + 41
               A(K,L) = CMPLX(MTF(I,J) * CIRCLE(I,J))
  300    CONTINUE
C
C     Inverse Fourier Transform matrix A
C
        IA1 = 80
        IA2 = 80
        N1 = 80
        N2 = 80
        N3 = 1
        IJOB = -1
        CALL FFT3D(A,IA1,IA2,N1,N2,N3,IJOB,IWK,RWK,CWK)
C
C    Transpose matrix quadrants to get reasonable picture
C
        DO 600 J = 1,40
           DO 600 I = 1,40
              F(I,J) = A(I+40,J+40)
  600    CONTINUE
        DO 610 J = 41,80
           DO 610 I = 1,40
              F(I,J) = A(I+40,J-40)
  610    CONTINUE
        DO 620 J = 1,40
           DO 620 I = 41,80
              F(I,J) = A(I-40,J+40)
  620    CONTINUE
        DO 630 J = 41,80
           DO 630 I = 41,80
              F(I,J) = A(I-40,J-40)
  630    CONTINUE
C
C     Write matrix into file
C
        DO 400 J = 1,80
           DO 400 I = 1,80
              D(I,J) = CMPLX(F(I,J))
              WRITE (10,*) CABS(D(I,J))
  400    CONTINUE
C
C    Take a slice of the cylinder to examine slope
C
        DO 410 I = 1,80
         WRITE (12,*) I,CABS(D(39,I))
  410    CONTINUE
        CLOSE (10)
        CLOSE (11)
        CLOSE (12)
        END
```

Bibliography

1. Bueche, Frederick J. College Physics (Seventh Edition). New York: McGraw Hill Book Company, 1979.

2. Bunner, Alan N. "Optical Arrays for Future Astronomical Telescopes in Space," Infrared, Adaptive, and Synthetic Aperture Optical Systems, SPIE 643: 180-188 (1986).

3. Carleton, Nathaniel P. and William F. Hoffmann. "The Multiple Mirror Telescope," Physics Today, 31: 30-37 (September 1978).

4. Evans, Howard E. II and James J. Lange. "Electro-Optical Space Systems Technology," Course notes for PHYS 621. School of Engineering, Air Force Institute of Technology (AU), Wright-Patterson AFB, OH, January 1989.

5. Evans, Howard E. II and James J. Lange. "Elements of Remote Sensing," Course notes distributed in PHYS 521, Space Surveillance. School of Engineering, Air Force Institute of Technology (AU), Wright-Patterson AFB, OH, May 1989.

6. Fender, Janet S. "Phased Array Optical Systems," Infrared, Adaptive, and Synthetic Aperture Optical Systems, SPIE 643: 122-128 (1986).

7. Fender, Janet S. "Synthetic Apertures: An Overview," Synthetic Aperture Systems, 440: 2-7 (1984).

8. Fenno, Charles. Class handout distributed in COMM 685, Communication for Managers and Analysts. School of Systems and Logistics, Air Force Institute of Technology (AU),Wright-Patterson AFB, OH, April 1989.

9. Gaskill, Jack D. Linear Systems, Fourier Transforms, and Optics. New York: John Wiley and Sons, 1978.

10. Golay, Marcel J. E. "Point Arrays Having Compact, Nonredundant Autocorrelations," Journal of the Optical Society of America, 61: 272-273 (February 1971).

11. Harvey, James E. and Richard A. Rockwell. "Performance Characteristics of Phased Array and Thinned Aperture Optical Telescopes," Optical Engineering, 27: 762-768 (September 1988).

12. Joyce, Richard R. "Indium Antimonide Detectors for Ground-Based Astronomy," Proceedings of SPIE 443: 50-58 (1983).

13. Morlan, Bruce H. Class lectures during OPER 571, Operations Research I. School of Engineering, Air Force Institute of Technology (AU), Wright-Patterson AFB, OH, July-September 1988.

14. Ravindran, A. and others. Operations Research. New York: John Wiley and Sons,Inc.,1987.

15. Readhead, Anthony C. S. "Radio Astronomy by Very-Long-Baseline Interferometry," Scientific American,246: 52-61 (June 1982).

16. Reilander, Robert T. Incoherent Multiple Aperture Optical Imaging systems: Analysis and Design. MS Thesis AFIT/GSO/ENP/87D-2. School of Engineering, Air Force Institute of Technology (AU), Wright-Patterson AFB, OH, December 1987 (AD-A189).

17. Robinson, Leif J. "Update: Telescopes of the Future," Sky and Telescope, 72: 23-24 (July 1986).

18. Schnabel, James J. Jr. and others. Modulation Transfer Function (MTF) Measurement Techniques for Lenses and Linear Detector Arrays, NASA Technical Publication TM 86168 (N85 19812) Goddard Space Flight Center, MD (October 1984).

19. Schwartzchild, Bertram M. "Large New-Technology Optical Telescopes Proposed," Physics Today, 34: 17-20 (August 1981).

20. Smith, Warren J. Modern Optical Engineering. New York: McGraw Hill Book Company, 1966.

21. Wolfram, Stephen. Mathematica. New York: Addison-Wesley Publishing Company, Inc.,1988.

VITA

Major Konrad S. Gruca [redacted] He graduated from Gordon Technical High School in 1974 and attended the United States Air Force Academy, from which he received a Bachelor of Science in Chemistry in May, 1978. He attended Undergraduate Pilot Training at Vance AFB, OK, staying on as a T-38 instructor. In 1983, he went to RAF Alconbury, England, as an RF-4C Reconnaissance pilot, served eighteen months as an Air Liaison Officer in Stuttgart, West Germany, and concluded his European tour in April, 1988, as a Flight Commander and instructor pilot in the RF-4C at Zweibrucken AB, Germany. He reported to AFIT in May, 1988.

UNCLASSIFIED
SECURITY CLASSIFICATION OF THIS PAGE

REPORT DOCUMENTATION PAGE

Form Approved
OMB No. 0704-0188

1a. REPORT SECURITY CLASSIFICATION UNCLASSIFIED	1b. RESTRICTIVE MARKINGS
2a. SECURITY CLASSIFICATION AUTHORITY	3. DISTRIBUTION/AVAILABILITY OF REPORT Approved for public release; distribution unlimited
2b. DECLASSIFICATION/DOWNGRADING SCHEDULE	
4. PERFORMING ORGANIZATION REPORT NUMBER(S) AFIT/GSO/ENP/89D-3	5. MONITORING ORGANIZATION REPORT NUMBER(S)
6a. NAME OF PERFORMING ORGANIZATION School of Engineering 6b. OFFICE SYMBOL (If applicable) AFIT/ENP	7a. NAME OF MONITORING ORGANIZATION
6c. ADDRESS (City, State, and ZIP Code) Air Force Institute of Technology Wright-Patterson AFB OH45433-6583	7b. ADDRESS (City, State and ZIP Code)
8a. NAME OF FUNDING/SPONSORING ORGANIZATION 8b. OFFICE SYMBOL (If applicable)	9. PROCUREMENT INSTRUMENT IDENTIFICATION NUMBER
8c. ADDRESS (City, State, and ZIP Code)	10. SOURCE OF FUNDING NUMBERS PROGRAM ELEMENT NO. / PROJECT NO. / TASK NO / WORK UNIT ACCESSION NO.
11. TITLE (Include Security Classification) BROADBAND INCOHERENT IMAGING USING MULTIPLE APERTURE OPTICS	
12. PERSONAL AUTHOR(S) Gruca, Konrad S., Maj, USAF	
13a. TYPE OF REPORT MS Thesis 13b. TIME COVERED FROM _____ TO _____ 14. DATE OF REPORT (Year, Month, Day) 1989 December 15. PAGE COUNT 99	
16. SUPPLEMENTARY NOTATION	
17. COSATI CODES FIELD: 20 / GROUP: 6 / SUB-GROUP:	18. SUBJECT TERMS (Continue on reverse if necessary and identify by block number) Multiaperture, Incoherent Imaging, Synthetic Aperture
19. ABSTRACT (Continue on reverse if necessary and identify by block number) Thesis Advisor: James D. Targove, Capt, USAF	
20. DISTRIBUTION/AVAILABILITY OF ABSTRACT ☒ UNCLASSIFIED/UNLIMITED ☐ SAME AS RPT. ☐ DTIC USERS	21. ABSTRACT SECURITY CLASSIFICATION UNCLASSIFIED
22a. NAME OF RESPONSIBLE INDIVIDUAL James D. Targove, Capt, USAF	22b. TELEPHONE (Include Area Code) (513)255-2012 22c. OFFICE SYMBOL AFIT/ENP

DD Form 1473, JUN 86 *Previous editions are obsolete.*

SECURITY CLASSIFICATION OF THIS PAGE
UNCLASSIFIED

The theoretical resolution of a multiple mirror telescope can be studied through its Modulation Transfer Function (MTF). Using the figure of merit that the mirrors be moved apart in a manner that would maximize the spatial frequency at which the first zero appears in the MTF, this thesis studied the use of MTF information from multiple wavelengths to delay the appearance of an interior zero in the overall MTF. This would allow the mirrors to be moved further apart and thereby increase the spatial frequency at which the first zero appears in the MTF, thus increasing the resolving capability of the system.

Symmetrical configurations from three to six mirrors were studied. Each configuration was initially manually optimized at three microns, then the system was studied at a three to five micron range to see if the MTF information from other wavelengths would delay the appearance of an interior zero in the overall system MTF. An optimization routine was also employed to see if there were other, nonsymmetrical, mirror configurations that could possibly yield a better theoretical resolution than their symmetrical counterparts.

The various findings throughout the research are detailed. The results are presented as a function of increase in theoretical resolution from the single, three micron wavelength compared to the multiple, three-to five micron wavelength MTF of the system studied. In general, even-numbered symmetrical configurations showed a five to fifteen percent improvement in the MTF, while odd-numbered symmetrical configurations showed no increase in resolution from the single wavelength to broadband wavelength. The optimization routine, in general, yielded an increase in resolution when compared to a symmetrical system with the same number of mirrors.